Chemical Science

ROYAL SOCIETY OF CHEMISTRY

REVIEW

View Article Online
View Journal | View Issue

Cite this: *Chem. Sci.*, 2026, **17**, 4881

Interfacial failure mechanisms and design principles in solid-state sodium batteries

Mingyue Wang,†* Qing Zhong,† Yue Wang,† Xu Liu, Dongyang Zhang* and Shujiang Ding *

Solid-state sodium batteries (SSSBs) have attracted increasing attention as a promising alternative for large-scale energy storage owing to their intrinsic safety, material abundance, and potential cost advantages. Significant progress has been made in developing diverse solid-state electrolytes, including polymers, inorganic ceramics, and hybrid systems, many of which exhibit impressive bulk ionic conductivity. However, the translation of these materials-level properties into durable, high-performance solid-state sodium batteries remains limited, indicating that bulk ion transport alone does not govern practical cell behavior. In this review, we adopt an interface-centered and issue-driven perspective to analyze the key challenges in SSSBs. Rather than providing a materials-category-based summary, we focus on dominant interfacial failure mechanisms and their sodium origins. Chemical and electrochemical instability, electrical blocking associated with space-charge effects and grain boundaries, mechanical degradation arising from elastic and thermal mismatch, and defect-assisted sodium dendrite penetration are discussed within a unified mechanistic framework. These interfacial processes are shown to be intrinsically coupled, collectively controlling effective ion transport, critical current density, and long-term cell stability. Building on this understanding, we critically assess why high bulk ionic conductivity has not translated into robust full-cell performance and emphasize the limitations of conductivity as a single performance metric. We further discuss general design principles for interface engineering across different electrolyte families and revisit lessons from technologically mature sodium battery systems to clarify realistic pathways toward practical implementation. By linking interfacial chemistry, defect physics, and mechanical properties, this Review aims to provide a coherent framework and forward-looking guidance for the rational design of next-generation SSSBs.

Received 28th November 2025
Accepted 24th January 2026

DOI: 10.1039/d5sc09313a

rsc.li/chemical-science

School of Chemistry, Engineering Research Center of Energy Storage Materials and Devices, Ministry of Education, National Innovation Platform (Center) for Industry-Education Integration of Energy Storage Technology, Xi'an Jiaotong University, Xi'an 710049, P. R. China. E-mail: mywang@xjtu.edu.cn; dingsj@xjtu.edu.cn; zdysun@xjtu.edu.cn

† These authors contributed equally.

Mingyue Wang

Mingyue Wang is currently an associate professor at Xi'an Jiaotong University, China. She obtained her PhD degree from the Northwestern Polytechnical University in 2020 and was a visitor at Hong Kong University of Science and Technology. Her research interests lie in the design and modification of key materials for secondary ion batteries, with a specific focus on the interfacial characteristics and reaction mechanisms underlying energy storage and ion transfer kinetics.

Dongyang Zhang

Dongyang Zhang is currently an associate professor at Xi'an Jiaotong University, China. He obtained his PhD degree from Xi'an Jiaotong University in 2020. He mainly focuses on the study of lithium/sodium ion batteries, including electrode materials, battery electrolytes, and electrode polymer binders. He conducts studies on material design and synthesis, structure and performance, as well as functions and mechanisms. So far, he has published over 30 research papers.

1 Introduction

1.1 From liquid electrolytes to solid electrolytes

Rechargeable secondary batteries have become a crucial energy storage and conversion solution supporting renewable energy integration over the past decade.[1–3] Among the various types, lithium-ion batteries (LIBs) stand out due to their superior energy density, high power delivery, and extended cycling stability, leading to their extensive use in everyday applications like mobile devices and electric transportation. Despite their success, the continued advancement of LIBs is constrained by several limitations—such as scarce lithium reserves, geographically imbalanced lithium ore distribution, and increasing raw material expenses (Fig. 1a)—posing barriers to long-term scalability.[4,5] These challenges, coupled with the rising demand for efficient energy storage across multiple industries, have accelerated research into alternative battery chemistries beyond conventional lithium-ion systems.[6,7] Recently, sodium-based batteries have emerged as a promising candidate, drawing significant scientific and industrial interest due to their cost-effectiveness, the widespread availability of sodium, and operational mechanisms analogous to those of lithium-ion technologies.[8,9] While sodium-ion batteries (SIBs) generally exhibit lower theoretical energy densities compared to LIBs owing to the greater atomic mass of sodium, they offer compelling benefits for large-scale applications such as grid-level energy storage, where safety, longevity, and economic feasibility are prioritized over maximum energy density.[10,11]

The electrolyte is a critical component in sodium batteries, serving as the medium for sodium ion transport between the cathode and anode, thereby significantly affecting the energy density and rate performance of batteries. Electrolyte systems are typically classified into three types: aqueous, organic liquid, and solid-state electrolytes (SSEs).[12] Although aqueous electrolytes offer advantages such as high safety and stable cycling behavior, their narrow electrochemical stability window limited by water decomposition restricts the operating voltage to below 2 V, which inherently limits the achievable energy density.[13,14] Only under highly concentrated salt conditions, for example with 17 mol per L $NaClO_4$, can voltages beyond 2 V be attained, leading to the failure of achieving practical scalability of the aqueous systems.[15] Similar to those in lithium batteries, organic liquid electrolytes based on carbonate or ether solvents are commonly employed in sodium batteries.[16,17] Early research primarily focused on carbonate solvents like ethylene carbonate (EC) and propylene carbonate (PC), owing to their high dielectric constants and wide electrochemical windows.[18] By 2014, researchers had demonstrated that by tailoring the solvation structure of ether-based electrolytes, reversible co-intercalation of Na^+ ions along with ether molecules into graphite anodes could be achieved—a process not feasible with conventional carbonate electrolytes.[19] Moreover, ether-based electrolytes exhibit superior low-temperature performance and high-rate capability due to their strong reductive stability and low desolvation energy.[20] Despite ongoing advancements in liquid electrolyte formulations, the inherent flammability and thermal instability of organic electrolytes remain major concerns, often leading to thermal runaway and associated safety hazards in real-world applications. Numerous incidents in recent years—including fires and explosions during battery operation or charging—have been attributed to such risks, particularly under abusive conditions involving mechanical damage (*e.g.*, crushing or puncture), electrical abuse (*e.g.*, overcharging or short circuits), or excessive heat buildup, as shown in Fig. 1b.[21,22]

SSEs have emerged as a promising substitute for conventional liquid electrolytes, offering enhanced safety and improved electrochemical performance in battery systems.[23] Notably, β''-Al_2O_3 (BASE) solid electrolytes represent one of the earliest and most technologically mature sodium-ion conducting ceramics. Since the 1960s, BASE has been successfully employed in high-temperature molten sodium batteries, including Na–S, Na–$NiCl_2$ (ZEBRA), and Na–$FeCl_2$ systems, where it serves as a robust separator enabling fast Na^+ transport at operating temperatures of 250–350 °C.[24] These battery systems have reached commercial deployment for stationary energy storage, highlighting the exceptional chemical stability, high ionic conductivity, and long-term reliability of BASE electrolytes under harsh operating conditions. In recent years, extensive research has led to the development of various SSE types aimed at broadening the applicability of SSSBs.[25,26] Currently, SSEs for sodium batteries are primarily categorized into inorganic, organic (polymer) and inorganic–organic types (Fig. 1c), and the corresponding characteristics are summarized in Fig. 1d.[27,28] However, achieving both effective interface contact and chemical stability of the electrolyte–electrode interface is vital for high-performance SSSBs. Two central challenges therefore dominate the design of efficient SSSBs: (i) developing SSEs with high ionic conductivity at ambient temperatures, and (ii) engineering well-matched electrode–electrolyte interfaces.[29–31] In recent years, substantial progress has been achieved in boosting ionic conductivity through compositional modifications, composite integration, and innovative structural designs, with some advanced SSEs now

Shujiang Ding

Shujiang Ding is currently a professor at Xi'an Jiaotong University, China. He obtained his PhD degree from the Institute of Chemistry, Chinese Academy of Sciences in 2007. His current research focuses on the design and fabrication of polymer/inorganic nanocomposite materials, with a particular focus on their application in electrochemical energy storage systems such as lithium/sodium ion batteries, lithium–sulfur batteries, solid-state batteries, fuel cells, and lithium-ion battery recycling, as well as in sensor technology. He has published more than 160 papers.

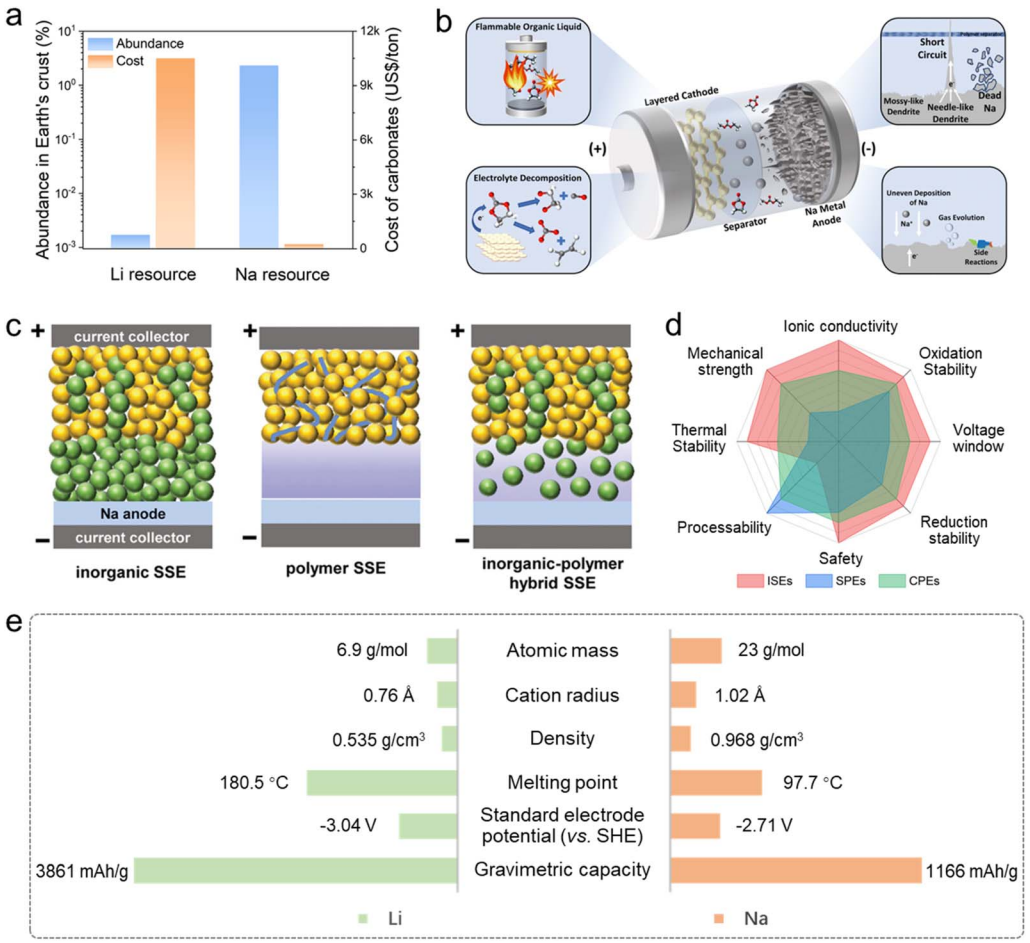

Fig. 1 (a) Abundance and costs of Li and Na resources. (b) Challenges in sodium batteries arising from organic liquid electrolytes.[35] Copyright 2023, The Royal Society of Chemistry. (c) Schematic diagram of inorganic SSE, polymer SSE and inorganic–polymer hybrid SSE based SSMBs.[36] Copyright 2023, Wiley-VCH. (d) Characteristics of ISEs, SPEs and composite polymer electrolytes (CPEs). (e) Comparison of physicochemical properties between Li and Na elements.

reaching conductivities comparable to those of liquid electrolytes.[32–34]

1.2 Similarities and differences with solid-state Li batteries

Owing to the similar electrochemical properties between lithium and sodium, SSSBs exhibit numerous functional similarities with solid-state lithium batteries (SSLBs). As a result, much of the fundamental understanding and experimental methodologies developed for SSSBs over recent years can be partially adapted to accelerate the advancement of SSSB technology.[37,38] Similar to their lithium counterparts, a typical SSSB consists of an anode, an SSE and a cathode. The working principles rely on the directional movement of cations coupled with redox reactions to enable energy storage and delivery.[39] The SSE functions as both an ionic conductor, facilitating Na^+ ion transport between electrodes, and as a physical barrier that prevents electrical shorting.[40,41] Oxidation occurs at the anode, releasing electrons into the external circuit and generating Na^+ ions that migrate through the SSE toward the cathode. At the cathode, these ions undergo electrochemical insertion into the host lattice, completing the energy release process.

Although SSSBs operate on the same "rocking chair" principle as SSSBs, and many similar materials for electrodes and electrolytes developed for SSSBs can be applied to SSSBs, significant distinctions exist between the two systems. These differences primarily stem from the distinct physicochemical characteristics of sodium and lithium, as illustrated in Fig. 1e. One of the most influential factors is the ionic radius, which directly affects ion diffusion kinetics and storage mechanisms. The larger ionic radius of Na^+ (1.02 Å) compared to Li^+ (0.76 Å), along with its lower charge density, makes Na^+ migration more challenging within the crystal lattice of SSEs.[42] For instance, in inorganic solid electrolytes such as NASICON-type materials, wider conduction pathways are required for Na^+ to avoid increased energy barriers caused by steric constraints.[43,44] Moreover, certain materials widely used in SSSBs—such as the $LiCoO_2$ cathode and $Li_7La_3Zr_2O_{12}$ electrolyte—are not suitable for use in SSSBs.[45,46] A major hurdle in the development of SSSBs is the optimization of electrode–electrolyte interfaces. The larger size of Na^+ ions promotes the formation of a dense and thick space charge layer at the interface, leading to significantly higher interfacial impedance compared to Li^+-based systems. In composite organic-inorganic electrolytes, the transfer of Na^+

across the internal phase boundary faces a greater energy barrier due to weaker coordination between Na^+ and the polymer matrix, as well as reduced lattice compatibility with inorganic fillers—both of which are less favorable than in lithium systems—resulting in a pronounced ion transport bottleneck.[47,48] Additionally, mismatches in thermal expansion coefficients between sodium-based components are more pronounced; for example, the difference between sodium-β-Al_2O_3 and metallic sodium can increase the likelihood of interfacial delamination under thermal cycling, further exacerbating impedance growth.[49,50] Chemical compatibility between the electrolyte and electrodes is another concern, for example, sulfide-based SSEs tend to react adversely with metallic sodium anodes.[51,52] All in all, while SSSBs share fundamental similarities with SSSBs—enabling the leveraging of existing research—their unique challenges arising from the physicochemical properties of sodium make interface engineering and material selection more complex. These distinctions demand focused attention to overcome the obstacles impeding the performance and commercialization of SSSBs.

Despite the rapidly growing body of literature on solid-state electrolytes for sodium batteries, a number of fundamental questions remain insufficiently addressed. In particular, the performance gap between impressive ionic conductivity values reported for many sodium solid electrolytes and the poor durability and rate capability of full solid-state sodium batteries persists as a central bottleneck. This discrepancy suggests that materials chemistry alone is not the limiting factor, and that interfacial phenomena, mechanical compatibility, and sodium-specific electrochemical behaviors play a decisive role in determining practical cell performance.[53,54] In this Review, rather than providing a purely materials-category-based summary, we adopt a problem-driven and concept-oriented perspective to critically analyze solid-state sodium battery systems. We emphasize three overarching themes. First, we examine the fundamental differences between sodium and lithium solid-state batteries that extend beyond simple ionic radius considerations, with particular focus on interfacial chemistry, space-charge effects, and failure mechanisms unique to sodium systems. Second, we critically assess why high bulk ionic conductivity has not translated into robust full-cell performance, highlighting the limitations of conductivity as a single performance metric and underscoring the importance of interfacial resistance, critical current density, and realistic full-cell validation. Third, we revisit technologically mature systems such as β″-Al_2O_3-based high-temperature molten sodium batteries, extracting key lessons from their long-term success and discussing the challenges associated with translating these advantages to lower-temperature solid-state configurations. By integrating insights across organic, inorganic, and hybrid electrolyte systems, and by explicitly linking ion transport, interfacial chemistry, and mechanical properties, this review aims to provide a coherent framework for understanding the persistent challenges in solid-state sodium batteries. We further identify near-term research priorities and realistic technological pathways, clarifying where progress is fundamentally materials-limited *versus* engineering-limited, and highlighting application scenarios in which sodium-based solid-state systems may offer advantages over their lithium counterparts.

2 Mechanisms and challenges of solid-state electrolytes

2.1 Transport mechanisms of Na-ions in solid-state electrolytes

The transport behavior of sodium ions in SSEs directly determines the overall ionic conductivity and electrochemical performance of the SSSBs. Typically, the ion transport mechanism is closely tied to the specific type of SSE and temperature,[25,55] as provided in Fig. 2a. Clarifying these region-specific transport mechanisms is not only essential for understanding the fundamental principles of ion conduction in solid systems, but also provides critical guidance for the structural design and performance optimization of SSEs.

2.1.1 Inorganic species. In crystalline inorganic electrolytes, ion conduction is primarily governed by the concentration of mobile Na^+ ions per unit volume and the presence of structural defects such as vacancies (missing ions) or interstitial sites, which can arise from atomic substitutions.[56,57] According to the Schottky and Frenkel defect models, the transport of sodium ions is actually achieved *via* random hopping between vacant lattice positions, direct interstitial jumps, or exchange between interstitial and substitutional sites,[35,58] as illustrated in Fig. 2b and c. For high ionic conductivity, several factors are essential: a sufficient number of charge carriers (Na ions), accessible neighbouring sites or defects, low energy barriers for ion movement, and well-defined conduction pathways.[59,60] The ionic conductivity (σ) of crystalline inorganic SSEs is commonly expressed through the Arrhenius equation:[61]

$$\sigma = \sigma_0 e^{(-E_A/k_B T)} \quad (1)$$

Here, σ_0 represents the pre-exponential factor, which includes contributions such as charge carrier density; E_A denotes the activation energy for ion diffusion, reflecting the minimum energy required for ions to overcome conduction bottlenecks; T is the absolute temperature in Kelvin, which determines the process through which mobile sodium ions interact with the structural framework during the migration process; and k_B stands for the Boltzmann constant. Consequently, the overall conductivity is influenced by the diffusion barrier, operating temperature, and the pre-exponential factor—particularly the carrier concentration. The diffusion barrier typically corresponds to the energy needed to pass through narrow diffusion channels. Strategies such as increasing mobile ion concentration, minimizing steric hindrance, and engineering continuous diffusion networks can significantly enhance ionic conductivity.[62,63] During this process, mobile Na^+ ions dynamically interact with the surrounding disordered matrix, with mobility strongly dependent on thermal energy.

2.1.2 Organic species. Ion conduction in organic SSEs operates under a fundamentally different principle compared to inorganic crystalline materials. In these systems, sodium ion

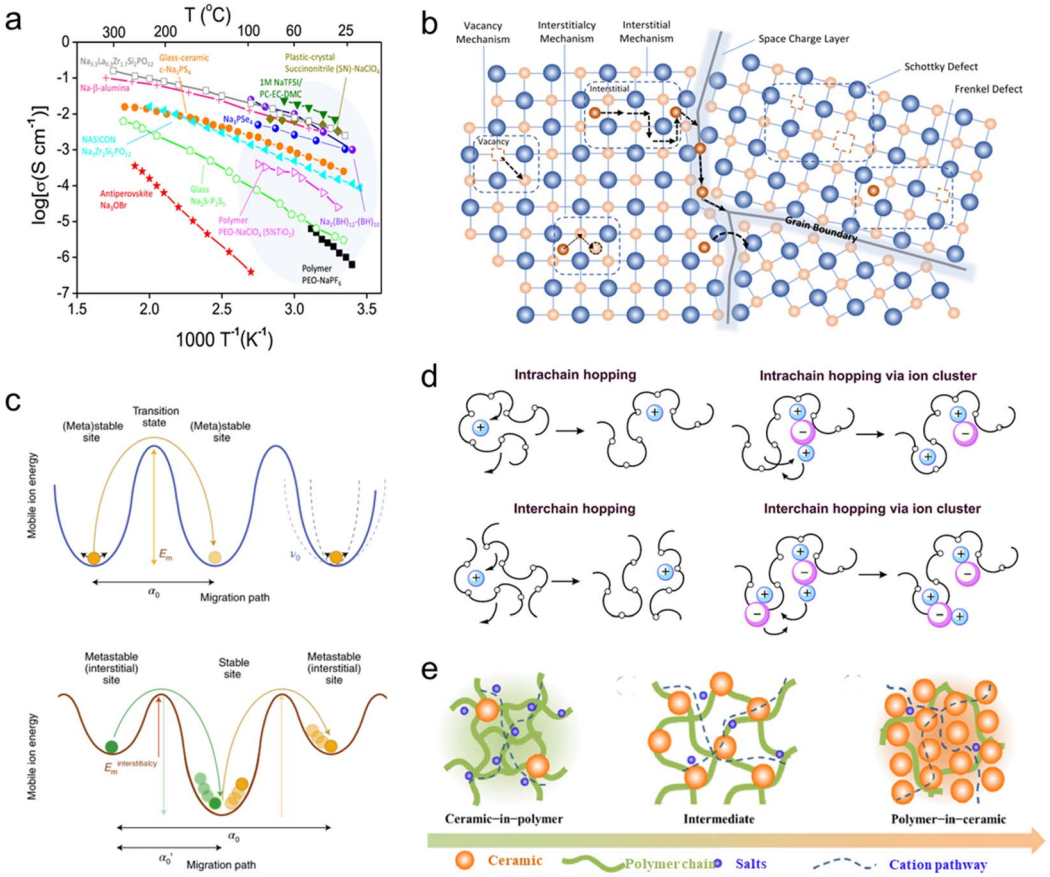

Fig. 2 (a) Temperature-dependent ionic conductivities of typical SSEs for sodium batteries.[25] Copyright 2018, Elsevier. (b) Na-ion transport mechanism in ISEs.[35] Copyright 2023, The Royal Society of Chemistry. (c) The energy profiles associated with cation migration *via* direct vacancy or interstitial hopping and correlated hopping.[69] Copyright 2022, Springer Nature. (d) Na-ion transport mechanism in SPEs[66] and (e) inorganic/organic hybrid SSEs.[70] Copyright 2015, The Royal Society of Chemistry. Copyright 2018, Elsevier.

transport is intimately linked to the segmental motion and flexibility of polymer chains, driven largely by the repeated coordination and de-coordination of Na^+ ions with polar functional groups along the polymer backbone. Common coordinating moieties such as ether oxygens, carbonyl groups, and nitrile functionalities can form transient bonds with sodium ions. When polymer chains undergo thermal motion like rotation and creep, these coordination bonds break and reform, enabling Na^+ ions to hop from one binding site to another, thereby facilitating ion migration (Fig. 2d).[64–66] The ionic conductivity of organic SSEs is often modelled by the Arrhenius equation (eqn (1)) or Vogel–Tammann–Fulcher (VTF) equation (eqn (2)):[36]

$$\sigma = \sigma_0 T^{-1/2} e^{-B/(T-T_0)} \quad (2)$$

in which B represents the pseudo-activation energy for conductivity, and T_0 is a reference temperature, typically around 50 K below the glass transition temperature (T_g). Most organic SSEs exhibit poor conductivity at room temperature owing to restricted chain mobility in highly ordered or crystalline domains. Enhancing conductivity in these systems can be achieved by reducing polymer crystallinity—thereby promoting greater segmental dynamics—and by increasing the number of free, dissociated Na^+ ions available for conduction.[67,68]

2.1.3 Organic–inorganic hybrid species. The hybrid organic–inorganic domain is created through the integration of the organic phase such as polymers with the inorganic phase like ionic conductors to construct a continuous and efficient ion transport network. The overall ionic conductivity of the hybrid system depends critically on the specific chemical composition and microstructural arrangement, typically described by VTF. Sodium ion transport relies on the cooperative interaction between both phases and their interfacial regions,[70,71] as shown in Fig. 2e. The inorganic phase serves as a rapid conduction scaffold, offering pathways with low activation energy for ion movement, while the organic matrix fills structural gaps and supports ion diffusion. At the interface, synergistic interactions can lead to the formation of optimized conduction layers that lower the energy barrier for ion transfer across phases, and in some cases, even promote the emergence of new conductive species.[72,73] Generally, such well-integrated composite electrolytes exhibit superior ionic conductivity compared to single-phase materials, effectively overcoming the limitations of low conductivity in organic components and poor interfacial compatibility in inorganic ones.

Beyond theoretical modelling, electrochemical impedance spectroscopy (EIS) is widely used to experimentally determine the ionic conductivity of SSEs. In this method, the SSE is placed between two ion-blocking electrodes (*e.g.*, stainless steel), allowing the calculation of σ using the formula:[74]

$$\sigma = \frac{I}{SR_t} \tag{3}$$

where I, S and R_t represent the thickness, cross-sectional area and total resistance of the electrolytes, respectively. The resulting conductivity from EIS measurements is referred to as apparent conductivity, as it accounts for contributions from both cations and anions. To evaluate the relative contribution of Na^+ ions, the ionic transference number (t_+) is introduced, defined as:

$$t_+ = \frac{\mu_+}{\mu_+ + \mu_-} \tag{4}$$

with μ_+ and μ_- denoting the mobilities of cations (Na^+) and anions, respectively. This parameter is crucial for assessing the efficiency of Na^+ transport in SSEs. The transference number can be determined *via* the steady-state current method using symmetric cells with sodium metal electrodes (Na/SSE/Na).[75] It is calculated according to:

$$t_+ = \frac{I_{ss}(\Delta V - I_0 R_0)}{I_0(\Delta V - I_{ss} R_{ss})} \tag{5}$$

in which I_{ss} is the steady-state current, I_0 represents the initial current, R_0 and R_{ss} are the initial and steady-state resistances, and ΔV denotes the applied constant potential (usually $\leq$10 mV). A higher t_+ value indicates more dominant Na^+ ion conduction. Inorganic SSEs typically achieve transference numbers approaching 126, reflecting nearly exclusive cationic conduction. In contrast, polymer-based SSEs usually have t_+ values below 0.5 due to the simultaneous and opposing migration of both Na^+ cations and anions.

2.2 Interfacial failure modes in solid-state sodium batteries

Although interfacial issues are widely recognized as the primary bottleneck in solid-state sodium batteries, their underlying mechanisms are often discussed in a fragmented and qualitative manner. In practice, interfacial failure rarely originates from a single factor; instead, it emerges from the coupled effects of interfacial chemistry, defect-mediated ion transport, and mechanical mismatch.[76] Sodium-specific properties—including its stronger reducing character, lower elastic modulus, and slower ion mobility compared to lithium—amplify these couplings and give rise to failure modes that are distinct from those in lithium-based solid-state systems. From a chemical perspective, many sodium solid electrolytes are thermodynamically unstable against sodium metal or high-voltage cathodes, leading to continuous interphase growth and increasing interfacial resistance.[77] Electrically, space-charge layers and grain boundary barriers dominate ion transport, explaining why high bulk ionic conductivity often fails to translate into high effective conductivity at the cell level. Mechanically, volume fluctuations during cycling and

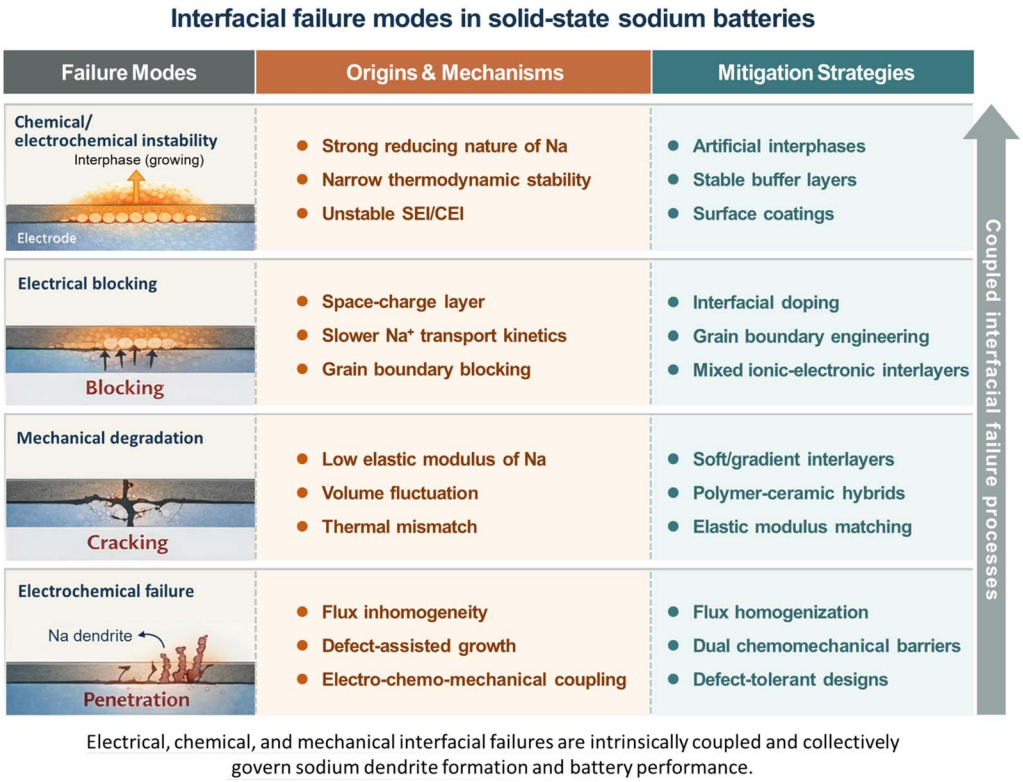

Fig. 3 Schematic framework illustrating dominant interfacial failure modes in solid-state sodium batteries. The framework emphasizes the coupled nature of interfacial chemistry, defect physics, and mechanical properties in determining practical battery performance.

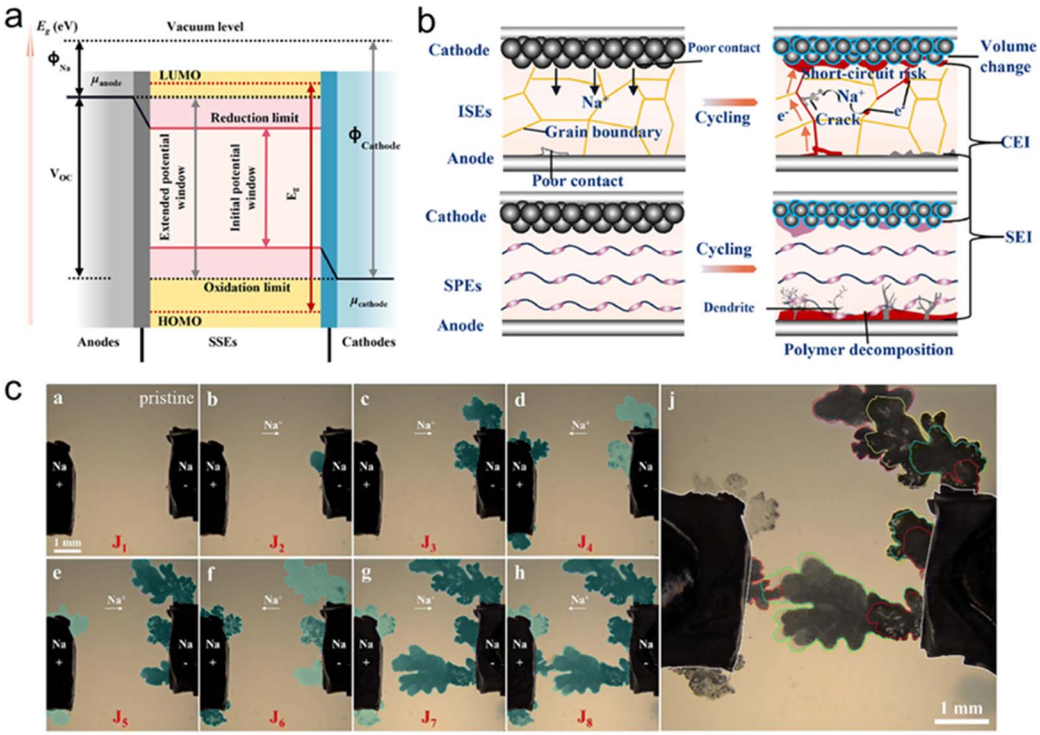

Fig. 4 (a) Schematic illustration of the open-circuit energy diagram for a SSSB. (b) Interface separation and dendrite growth in SSSBs.[92] Copyright 2024, Elsevier. (c) *In situ* growth of Na dendrites.[101] Copyright 2023, The Royal Society of Chemistry.

mismatched elastic moduli induce interfacial debonding and crack formation, which further localize current density and accelerate degradation. These chemical, electrical, and mechanical processes are intrinsically coupled and collectively promote electrochemical failure, such as sodium dendrite nucleation and penetration under practical current densities. Fig. 3 summarizes the dominant interfacial failure modes in solid-state sodium batteries, their sodium-specific origins, and corresponding mitigation strategies. This framework highlights that addressing interfacial challenges requires integrated design approaches rather than isolated materials optimization.

2.2.1 Chemical and electrochemical interfacial instability. Chemical and electrochemical instability at the electrode–electrolyte interface represents the earliest and most pervasive failure mode in solid-state sodium batteries. The degradation mechanisms of SSEs related to chemical and electrochemical stability mainly arise from undesirable chemical reactions with electrode materials and intrinsic decomposition occurring within certain voltage windows.[78,79] These processes contribute to a substantial rise in interfacial impedance and the depletion of active components. Compared to Li, Na shows stronger reducibility, which is more likely to result in the formation of an unstable SEI/CEI. The electrochemical stability window of an SSE is fundamentally linked to the energy difference (E_g) between its highest occupied molecular orbital (HOMO, analogous to the valence band) and lowest unoccupied molecular orbital (LUMO, corresponding to the conduction band).[80] As illustrated in Fig. 4a, thermodynamic compatibility at the interface depends on whether the chemical potential of the electrodes (μ_{anode} or $\mu_{cathode}$) lies within the HOMO–LUMO range. If μ_{anode} exceeds the LUMO level, reduction occurs at the anode interface; similarly, if $\mu_{cathode}$ falls below the HOMO level, oxidation takes place at the cathode side, leading to interlayer formation. In practice, however, the electrode potentials often exceed the electrochemical stability window of the electrolyte, triggering complex and persistent interfacial side reactions. This leads to the continuous formation of interphases such as the SEI and cathode–electrolyte interphase (CEI). For instance, inorganic solid electrolytes can react chemically with cathodes, producing resistive by-products like oxides or fluorides that hinder ion conduction pathways.[81] In contrast, organic solid electrolytes are prone to oxidative breakdown at high voltages or reductive decomposition when in contact with sodium metal anodes at low potentials, thereby undermining electrolyte integrity.[82] Such degradation phenomena cause a rapid increase in interfacial resistance and a marked reduction in ionic conductivity, ultimately impairing charge–discharge efficiency and reducing the cycle lifespan of the batteries.

2.2.2 Electrical blocking and space-charge-dominated transport. Beyond chemical decomposition and mechanical degradation, electrical blocking at solid–solid interfaces constitutes a critical yet frequently underestimated failure mode in solid-state sodium batteries. In many reported systems, high bulk ionic conductivity measured from dense electrolyte pellets does not translate into efficient ion transport at the cell level. Instead, ion migration is dominated by interfacial resistance arising from space-charge layers, grain boundary barriers, and electronically insulating interphases.[83] The formation of space-charge layers at electrode–electrolyte

interfaces is particularly pronounced in sodium-based systems. Owing to the larger ionic radius and lower mobility of Na^+ compared to Li^+, even modest interfacial potential gradients can induce substantial redistribution of charge carriers near the interface. This leads to sodium-ion depletion or accumulation zones that effectively block ion transport, resulting in a sharp increase in interfacial impedance.[84,85] In polycrystalline inorganic electrolytes such as NASICONs and oxides, similar blocking effects arise at grain boundaries, where compositional inhomogeneity, secondary phases, or defect segregation further hinder Na^+ migration. These electrical bottlenecks provide a compelling explanation for the widespread discrepancy between bulk conductivity and practical electrochemical performance.[86] Although many sodium solid electrolytes exhibit room-temperature conductivities exceeding 10^{-3} S cm^{-1}, the effective conductivity governing full-cell operation is often orders of magnitude lower. As a consequence, critical current densities remain limited, and stable sodium plating/stripping is difficult to sustain under practically relevant areal capacities. Importantly, electrical blocking effects are not static; they tend to intensify during cycling as interfacial reactions, mechanical damage, and defect accumulation further amplify local potential gradients and ion flux heterogeneity. Mitigating electrical blocking requires strategies that explicitly target interfacial ion transport rather than further optimization of bulk lattice conductivity. Promising approaches include interfacial doping to modify local defect chemistry, grain boundary engineering to reduce transport barriers, and the introduction of thin mixed ionic–electronic interlayers that homogenize sodium-ion flux while maintaining overall electrochemical stability.[87–90] These considerations underscore that overcoming electrical blocking is central to bridging the gap between impressive materials-level properties and durable, high-rate solid-state sodium battery performance.

2.2.3 Mechanical degradation and interfacial delamination. Generally, differences in composition and structure at the interface between the SSE and the electrode material may result in the generation of decomposition byproducts, which can result in mechanical failure to hinder either ionic or electronic conductivity.[91] This issue is far more intricate than the solid–liquid interface interactions observed in conventional liquid electrolyte batteries, as the inherent rigidity and limited flexibility of solid electrolytes can impose excessive mechanical stress on battery components. A significant mismatch in thermal expansion coefficients between the SSEs and adjacent electrodes may lead to interfacial stress build-up under temperature fluctuations, promoting delamination, as illustrated in Fig. 4b.[92–94] Inorganic SSEs, such as oxide- and halide-based materials, generally possess high thermal stability, with decomposition temperatures significantly exceeding those of organic electrolytes—some oxide ceramics remain stable above 1000 °C. Despite this, the interfacial reactions with the electrodes may be exacerbated at high temperatures.[95] In contrast, organic electrolytes, which have low thermal resistance, tend to soften or melt at high temperatures, resulting in decreased mechanical strength and a weakened ability to suppress dendrite growth, even accelerating side reactions at the electrode interface. Thermal stability failure causes the battery to lose its ion conduction function at extreme temperatures and may induce chain reactions, intensifying the risk of battery thermal runaway and endangering operational safety.[96,97] Mechanical degradation not only increases interfacial resistance but also accelerates chemical and electrochemical failure by locally amplifying current density.

2.2.4 Electrochemical failure: sodium dendrite nucleation and penetration. Sodium dendrite formation should be viewed as a coupled electrochemical failure mode rather than an isolated phenomenon. In solid-state sodium batteries, sodium dendrite formation is strongly coupled with structural defects such as cracks, pores, and grain boundaries within the electrolyte.[98,99] These defects locally distort the electric field and sodium-ion flux, leading to pronounced current focusing at defect tips. As a result, sodium ions preferentially migrate toward these regions, significantly lowering the nucleation barrier for metallic sodium deposition that evolves into needle-like dendritic structures.[100,101] Once sodium nucleates within defects, continued deposition generates local mechanical stress due to volumetric expansion, which further propagates cracks and enlarges existing defects. This electro-chemo-mechanical coupling establishes a positive feedback loop, whereby defect-assisted sodium growth accelerates electrolyte degradation, enables dendrite penetration and ultimately triggers internal short circuits, as shown in Fig. 4c.[101] Such behavior is particularly severe in sodium systems due to the lower elastic modulus of sodium metal, slower Na^+ transport kinetics, and higher chemical reactivity at defect-rich interfaces.

3 Solid-state electrolyte design

3.1 Organic solid-state electrolytes

Organic solid-state electrolytes (OSE) generally consist of an organic compound matrix and sodium salts.[102] Most polymer electrolytes still suffer from low ionic conductivity at room temperature and unsatisfactory Na^+ transference numbers, which significantly limit their practical application.[74,103,104] According to the type of organic matrix, OSE can mainly be divided into polymer SSEs and gel SSEs.

3.1.1 Polymer SSEs. SPEs primarily consist of a polymer matrix, either entirely free of or containing only trace amounts of liquid phases.[74,105] Owing to their low cost and excellent processability, polymer solid electrolytes are widely considered as one of the most promising candidates for commercial SSSBs.[106] Nevertheless, several obstacles hinder their widespread application, particularly their typically low ionic conductivity under ambient conditions (often below 10^{-5} S cm^{-1}) mainly due to the high T_g of the polymer framework that limits chain mobility.[107] To overcome this limitation, polymer electrolytes usually operate at elevated temperatures above T_g (usually 60–80 °C), where enhanced segmental mobility improves ion transport. However, such thermal activation decreases mechanical strength, resulting in a transition of the electrolyte from a solid to quasi-liquid state, thereby increasing safety risks such as dendrite penetration and thermal runaway. Consequently, current research focuses on

balancing high ionic conductivity with robust mechanical properties. Polymers with polar functional groups (*e.g.*, ether oxygen bonds and carbonyl groups) such as PEO and PVDF are commonly selected to strengthen sodium ion solvation, facilitating salt dissociation and ion mobility.[108] For example, a fluorinated polymer membrane (PCUF) was fabricated by chemically cross-linking a fluorinated MOF within a PVDF-HFP matrix, as displayed in Fig. 5a.[109] This synergy enables a high ionic conductivity of 2.59×10^{-4} S cm^{-1} at room temperature and achieves an exceptional Na^+ transference number of 0.910. During thermal degradation, PCUF releases fluorine-containing radicals that effectively quench reactive gas-phase radicals, interrupting combustion propagation. The intrinsic flame-retardant behavior raises the onset temperature of thermal decomposition, enhancing overall thermal stability (Fig. 5b). Beyond these representative systems, various polymer modification strategies—including fluorination, block copolymer design, and single-ion conducting architectures—have been explored to enhance sodium ion transport and interfacial stability. While these approaches can improve specific performance metrics, their fundamental trade-offs between ionic conductivity, mechanical strength, and electrochemical stability remain largely similar.[110–114]

3.1.2 Gel polymer electrolyte. Gel polymer electrolytes (GPEs) were initially proposed by Feuillade and Perche in 1975.[115] These electrolytes are constructed from a hybrid system comprising a polymer scaffold infused with a certain amount of liquid plasticizers or liquid electrolytes, forming a semi-solid composite structure.[102,116] To facilitate ion transport, low-viscosity plasticizers with high dielectric constants, such as carbonate-based solvents, are incorporated into the polymer matrix, establishing a cooperative conduction mechanism between the polymer and liquid phases.[117–120] This unique architecture allows GPEs to combine the superior safety features of SSEs with the high ionic conductivity typical of liquid electrolytes.[117,121] In contrast to conventional liquid electrolytes, GPEs mitigate leakage risks, thereby enhancing operational safety. Moreover, due to the presence of mobile liquid components, they

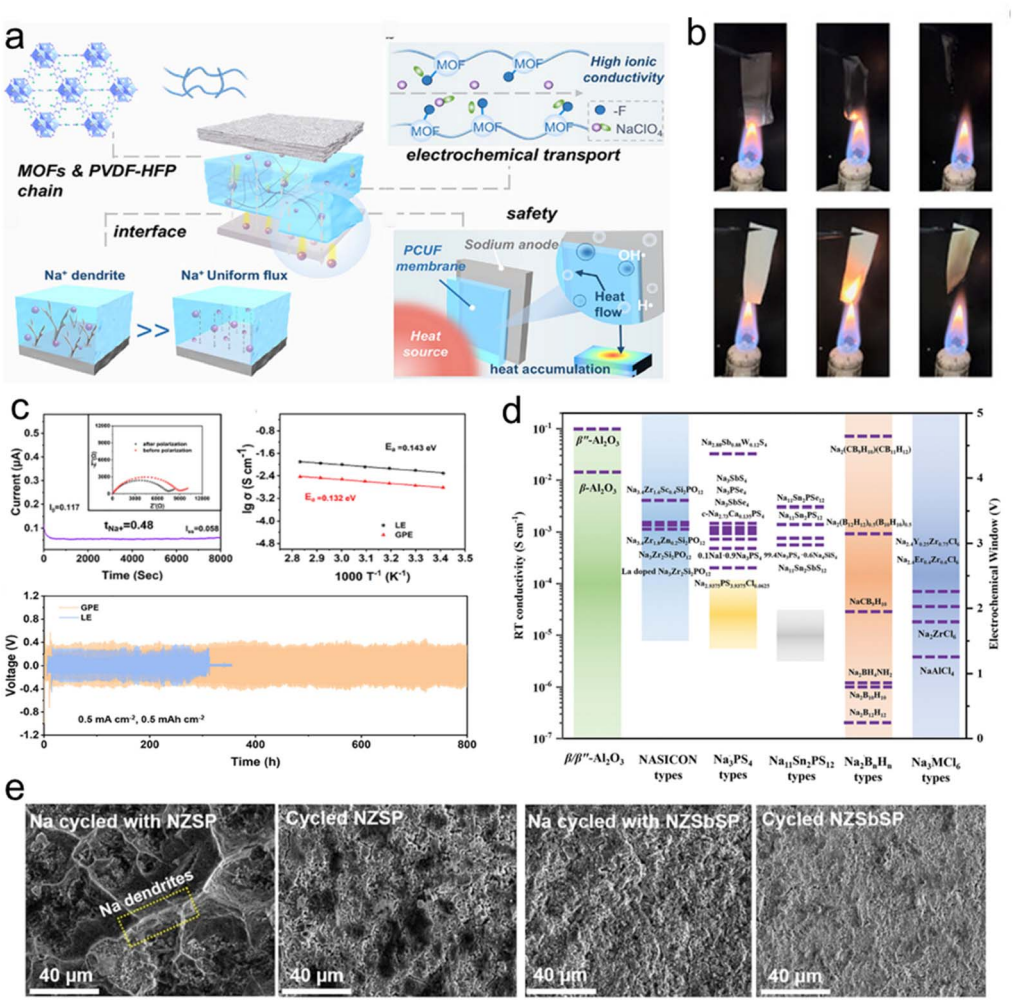

Fig. 5 (a) Schematic illustration of the design principle of PCUF SSEs. (b) Ignition experiments of PH and PCUF membranes.[109] Copyright 2025, Wiley-VCH. (c) Chronoamperometry curve and impedance variation, liner fitting plots for σ and voltage–time curves of the GPE and LE.[122] Copyright 2025, Wiley-VCH. (d) Ionic conductivities of ISSEs and the corresponding electrochemical stability windows.[61] Copyright 2023, Wiley-VCH. (e) SEM images of sodium metal, NZSP and NZSbSP in corresponding symmetric cells cycled at 60 °C.[127] Copyright 2025, Elsevier.

maintain a high ionic conductivity of $\sim 10^{-3}$ S cm^{-1} at room temperature, significantly outperforming SPEs. Despite these advantages, challenges remain, including insufficient mechanical strength and low Na^+ transference numbers (typically below 0.5). As a result, current research efforts focus on optimizing the trade-off between high ionic conductivity, mechanical robustness, and interfacial stability. Inspired by the capsule concept, Jiao *et al.* designed a capsule-inspired GPE based on triethyl phosphate (TEP) featuring a co-sustained release mechanism.[122] By embedding TEP within an insoluble ethoxylated trimethylolpropane triacrylate matrix alongside carbonate co-solvents, they effectively suppressed the corrosive interaction between TEP and the sodium metal anode while maintaining continuous flame-retardant functionality. The resulting electrolyte exhibited a high ionic conductivity of 1.24 mS cm^{-1}, a transference number of 0.48 for Na^+, and a stable electrochemical window of 4.68 V, as presented in Fig. 5c. Numerous gel polymer electrolyte designs have been reported with variations in polymer backbones, plasticizers, and cross-linking strategies.[123–126] Although these systems often achieve higher room-temperature conductivity than dry polymer electrolytes, their sodium-ion transference numbers and mechanical robustness remain limited, underscoring the persistent trade-off between ionic mobility and structural integrity.

3.2 Inorganic solid-state electrolytes

ISEs are based on inorganic compounds such as crystals and glassy states. They possess advantages such as high ionic conductivity, good chemical stability, and high pressure resistance. According to their crystal structure and composition, they can be classified into various types (Fig. 5d).

3.2.1 Na-β-alumina. Among various inorganic solid-state electrolytes for sodium batteries, Na-β-Al_2O_3, particularly β″-Al_2O_3, stands out as the most established and industrially validated material. Unlike most emerging solid electrolytes that remain confined to laboratory-scale demonstrations, β″-Al_2O_3 has been extensively used for decades in high-temperature molten sodium batteries, such as Na–S and Na–$NiCl_2$ systems as mentioned above.[24] In these configurations, the electrolyte operates at elevated temperatures (typically 250–350 °C), where its two-dimensional Na^+ conduction planes enable ionic conductivities exceeding 10^{-1} S cm^{-1}, supporting high power output and long cycle life. Na-β-alumina is a layered inorganic solid electrolyte based on aluminum oxide, which features an interlayer capable of hosting a large number of mobile sodium ions, contributing to relatively high room-temperature ionic conductivity.[128,129] Of these, β″-Al_2O_3 demonstrates superior ionic conductivity due to its higher Na^+ ion density within the two-dimensional conduction planes and an expanded unit cell volume that promotes easier ion movement.[130,131] As a result, single-phase β″-Al_2O_3 can achieve superior ionic conductivity under ambient conditions. However, pure β″-Al_2O_3 suffers from limited mechanical strength (with a fracture strength of 200 MPa) and poor thermodynamic stability, posing challenges for synthesis.[132] It tends to decompose into Al_2O_3 and Na-β-Al_2O_3 at elevated temperatures near 1500 °C.[103,133]

To improve both ionic conductivity and mechanical performance, various strategies have been explored, including the substitution of Al^{3+} with foreign cations such as Li^+, Mg^{2+}, Nb^{5+}, Ti^{4+} and Zr^{4+}, which modify the Na^+ content in the conduction layers.[134–140] For instance, Chen *et al.*[141] doped β-Al_2O_3 with a 0.5 wt% Cu^{2+} stabilizing agent, boosting ionic conductivity to 1.2×10^{-3} S cm^{-1}. They further introduced an In_2S_3 interlayer between the sodium anode and the electrolyte, forming a composite layer composed of an Na–In alloy and Na_2S that exhibited mixed ionic–electronic conductivity. This strategy improved interfacial electrochemical stability and enabled efficient Na^+ transport. Various aliovalent dopants and secondary phases have been introduced to stabilize the β″ phase and enhance ionic conductivity; however, these compositional optimizations do not fundamentally resolve the interfacial and mechanical challenges encountered in lower-temperature solid-state configurations.[142–146] Traditional solid-state synthesis of Na-β-Al_2O_3 typically involves high sintering temperatures and prolonged processing times, often leading to decomposition of the desired β″-Al_2O_3 phase. To overcome these limitations, alternative fabrication techniques such as co-precipitation, sol–gel processes, microwave-assisted heating, and mechanochemical synthesis have been developed.[139,144,147–152] Despite these advances, achieving highly homogeneous and conductive β″-Al_2O_3 remains difficult due to issues such as sodium volatilization, abnormal grain growth, moisture sensitivity from boundary-phase $NaAlO_2$ formation, and residual impurities.[59] Process improvements like the double-zeta sintering method and spark plasma sintering (SPS) can enhance densification; however, the former demands extreme temperatures (up to 1600 °C), while the latter requires expensive equipment, limiting scalability.[153–155]

3.2.2 NASICONs. NASICON-type electrolytes, typically represented by the general formula $Na_{1+x}Zr_2Si_xP_{3-x}O_{12}$, are among the most extensively studied inorganic solid electrolytes for sodium batteries. Their three-dimensional anionic framework enables isotropic Na^+ transport, offering a fundamental structural advantage over layered conductors such as β″-Al_2O_3.[156–158] As a result, NASICON materials can achieve room-temperature ionic conductivities in the range of 10^{-4}–10^{-3} S cm^{-1} and exhibit good chemical stability toward a variety of cathode materials.[159–161] Despite these favorable bulk properties, the practical performance of NASICON-based solid-state sodium batteries remains limited. A recurring observation is the pronounced discrepancy between high bulk ionic conductivity and poor effective conductivity at the cell level.[162,163] Grain boundary resistance, interfacial instability against sodium metal, and the formation of resistive interphases collectively dominate ion transport, leading to low critical current densities and premature cell failure.[164–166] These limitations highlight that interfacial processes, rather than intrinsic lattice transport, govern the electrochemical performance of NASICON-based systems.

To address these challenges, extensive efforts have focused on compositional tuning and microstructural engineering. Representative approaches include aliovalent cation substitution to optimize lattice dimensions and grain boundary

chemistry, as well as surface modification strategies aimed at stabilizing the Na/NASICON interface.[167–169] Akbar *et al.* introduced Sb^{3+} into the NZSP lattice to tailor the crystal structure and facilitate ion mobility.[170] The resulting $Na_{3.1}Zr_{1.9}Sb_{0.1}Si_2PO_{12}$ (NZSbSP) exhibited a room-temperature ionic conductivity of 5.1×10^{-4} S cm^{-1}, improved structural stability, lowered grain boundary resistance, and effectively suppressed Na dendrite formation (Fig. 5e).[127] While such methods can reduce grain boundary impedance and improve cycling stability under moderate conditions, the resulting gains in full-cell performance remain incremental, and stable operation at practically relevant current densities remains difficult to achieve. Overall, NASICON-type electrolytes illustrate a broader challenge in solid-state sodium batteries: excellent bulk transport properties alone are insufficient to guarantee robust cell-level performance. Further progress will therefore depend less on continued optimization of lattice conductivity and more on interface engineering, defect control, and mechanically compliant cell architectures capable of sustaining uniform Na^+ flux under realistic operating conditions.

3.2.3 Sulfides. Sulfide-based solid electrolytes, including compounds such as Na_3MS_4 (M = P, Sb) and $Na_{11}Sn_2PS_{12}$, are characterized by exceptionally high ionic conductivity, ease of low-temperature densification, and favorable compatibility with sodium metal anodes.[171–174] The large ionic radii and moderate electronegativity inherent to sulfur atoms enable the formation of crystal architectures that support rapid ion transport. By employing techniques such as ball milling and thermal annealing, researchers can control phase purity and particle size, thereby minimizing interfacial resistance.[175,176] Additionally, halogen doping (*e.g.* using Cl^- and Br^-) has been shown to expand the electrochemical stability window, suppressing oxidative degradation at elevated voltages and enhancing both chemical and electrochemical robustness. While W-doped Na_3SbS_4 systems such as $Na_{2.88}Sb_{0.88}W_{0.12}S_4$ have been reported to exhibit total ionic conductivities above 3×10^{-2} S cm^{-1} at room temperature, these values include contributions from grain boundary effects, which can mask true bulk performance.[177] To reveal intrinsic conduction behavior, Königseriter *et al.* utilized low-temperature broadband impedance spectroscopy (down to −130 °C) to isolate the bulk conductivity of $Na_{2.9}Sb_{0.9}W_{0.1}S_4$ (Fig. 6a).[178] The measured bulk conductivity reached 1.8×10^{-3} S cm^{-1} even at low temperature, indicating strong inherent Na^+ migration. Currently, the

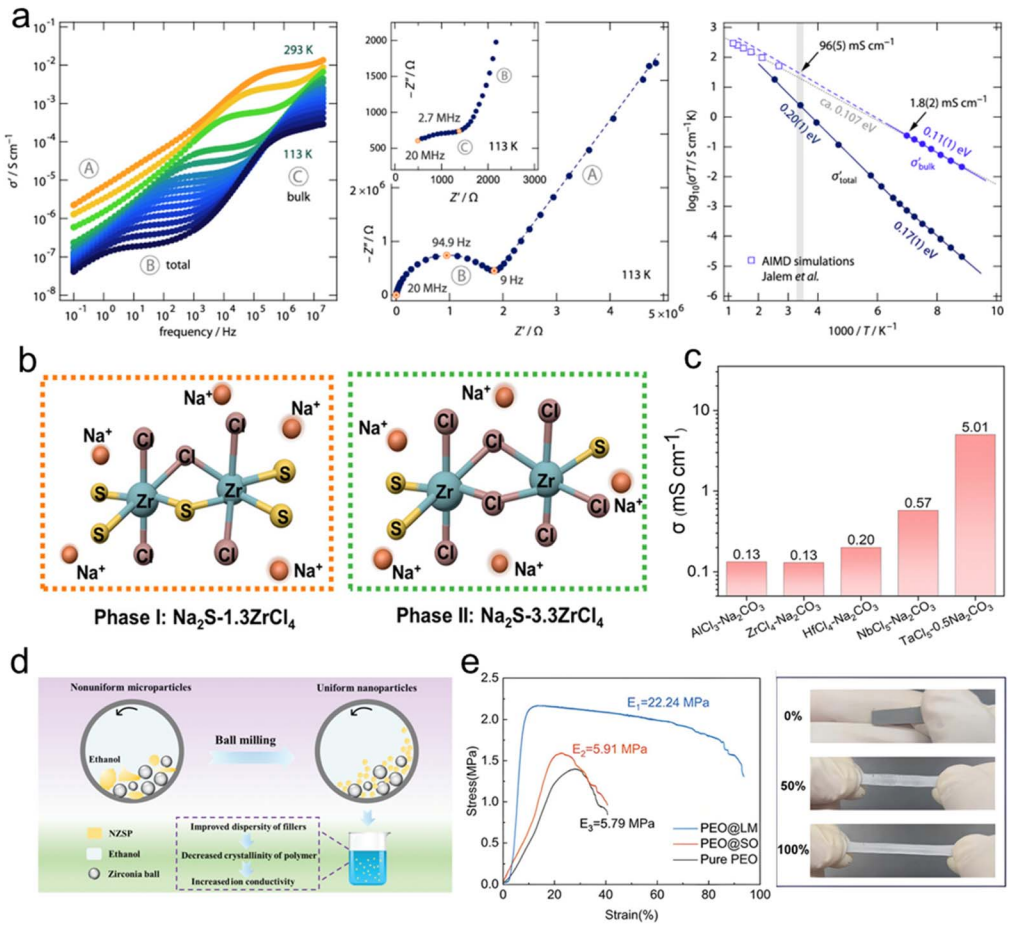

Fig. 6 (a) Conductivity of $Na_{2.9}Sb_{0.9}W_{0.1}S_4$.[178] Copyright 2025, American Chemical Society. (b) The scheme diagram of Na_2S–$1.3ZrCl_4$ SSEs and Na_2S–$3.3ZrCl_4$ SSEs.[180] Copyright 2025, Wiley-VCH. (c) RT ionic conductivities of MCl_y–xNa_2CO_3 samples (M = Ta, Nb, Hf, Zr, and Al).[181] Copyright 2025, The Royal Society of Chemistry. (d) Schematic illustration of the inorganic–organic hybrid SSE.[182] Copyright 2023, Wiley-VCH. (e) Mechanical properties of PEO@LM electrolyte.[183] Copyright 2024, Wiley-VCH.

main limitation to overall conductivity lies in grain boundary resistance rather than the bulk ionic transport itself, suggesting that targeted grain boundary engineering, such as interface modification or microstructural optimization, could significantly improve total conductivity.

Despite their outstanding ionic transport properties, sulfide-based electrolytes face significant challenges related to environmental instability. They are highly hygroscopic and prone to hydrolysis upon exposure to moisture, susceptible to oxidation when paired with high-voltage cathodes, and may undergo reduction reactions in contact with metallic sodium, severely restricting their practical deployment. Guo *et al.* introduced a multi-cation co-substitution strategy using Sn, W, Ca, and Ti at the Sb site in $Na_{3-\square}Sb_{1-4x}(SnWCaTi)_xS_4$.[179] This approach not only generated a high concentration of sodium vacancies but also increased the configurational entropy of the lattice, stabilizing the crystal structure. The resulting high-entropy electrolyte achieved a room-temperature ionic conductivity of 6.3×10^{-3} S cm^{-1} with a remarkably low activation energy of 0.15 eV. Besides, the ionic conductivity remained at 5.3×10^{-3} S cm^{-1} after 10 minutes in air with 50% relative humidity, and no structural degradation was observed, even upon direct exposure to water.

3.2.4 Other inorganic solid electrolytes. Apart from the above-mentioned electrolytes, other ISEs include halide, hydride, and hybrid inorganic electrolytes, *etc.*[184,185] While these systems may not yet match the ionic conductivity or electrochemical stability of mainstream counterparts, they offer distinct advantages that make them worthy of investigation. Halide-based sodium solid electrolytes, for instance, typically have the general formula $Na_{3-x}M_{1-x}M'_xX_6$, where M denotes a transition metal, lanthanide, or element from the boron/nitrogen group, M′ refers to Zr or its substituted variants, and X stands for one or more halogen elements.[35] Owing to the higher electronegativity of halide ions relative to O^{2-} and S^{2-}, halide electrolytes generally demonstrate superior oxidative stability. Among them, Na_2ZrCl_6 is the most studied chloride-based sodium conductor, albeit with a modest ionic conductivity of approximately 10^{-5} S cm^{-1}.[59] Recent studies indicate that incorporating oxygen can effectively improve ion transport.[186] Ruoff *et al.* employed mechanochemical synthesis using Na_2O to introduce oxygen into $NaAlCl_4$, achieving an optimized conductivity exceeding 1×10^{-4} S cm^{-1}.[187] Hydride-based electrolytes, which consist of Na^+ ions paired with complex anions such as $(BH_4)^-$, $(NH_2)^-$, $(AlH_4)^-$, and $(B_{10}H_{10})^{2-}$, are notable for their excellent reductive stability, mechanical flexibility, and low mass density.[188] In particular, borohydride-based SSEs exhibit favorable Na^+ conduction and good compatibility with metallic sodium anodes, though their application is limited by insufficient thermal and oxidative resilience.[189]

Growing attention has been directed toward hybrid inorganic systems. Dong *et al.* developed a new class of sulfide–chloride composite electrolytes (Na–Zr–S–Cl), yielding two phases: a chlorine-deficient form ($Na_2S{\cdot}1.3ZrCl_4$) and a chlorine-rich counterpart ($Na_2S{\cdot}3.3ZrCl_4$), as illustrated in Fig. 6b.[180] The latter delivered a high ionic conductivity of 4.89 $\times 10^{-4}$ S cm^{-1}, whereas the former showed superior chemical stability. Besides, the strategic integration of multiple anions to form amorphous frameworks has proven effective in simultaneously enhancing various electrolyte characteristics. Wang *et al.* synthesized a series of amorphous SSEs (MCl_y–xNa_2CO_3, M = Ta, Nb, Hf, Zr, Al) *via* high-energy ball milling.[181] The $TaCl_5{\cdot}1.2Na_2CO_3$ electrolyte achieved a high ionic conductivity of 1.11×10^{-3} S cm^{-1} at room temperature (Fig. 6c).

3.3 Inorganic–organic hybrid solid-state electrolytes

Inorganic–organic hybrid SSEs are composite systems formed by combining inorganic and organic components through either physical blending or chemical linkage, aiming to leverage the mechanical flexibility of polymers and the high ionic conductivity of inorganic phases to achieve complementary performance enhancements.[190] In these systems, polymers such as PEO and PVDF-HFP serve as continuous frameworks that provide structural flexibility and interfacial adaptability, while dispersed inorganic fillers, such as NASICON-type ceramics or sulfide-based conductors, act as ion-conducting reinforcements that establish efficient Na^+ transport networks, thereby enhancing overall ionic mobility.[191,192] By adjusting the filler loading, particle size, and dispersion homogeneity, the interfacial resistance between the two phases can be effectively minimized. For instance, Wang *et al.* engineered a bilayer architecture comprising a PEO layer adjacent to the sodium metal anode and a polyacrylonitrile (PAN)-based layer facing the high-voltage cathode,[182] as displayed in Fig. 6d. This approach introduced additional Na^+ conduction pathways and promoted segmental motion of PEO chains, yielding a thin (25 μm), lightweight (1.65 mg cm^{-2}) and mechanically robust (13.84 MPa) CPE with an ionic conductivity of 1.62×10^{-4} S cm^{-1}.

Although conventional inorganic fillers enhance stiffness to help suppress dendrite penetration, they often compromise material toughness and lack the ability to heal existing defects or mitigate "dead sodium" formation. To address this, modern designs exploit the rigidity of inorganic components to hinder dendrite propagation, while utilizing the elasticity of the organic phase to accommodate volume fluctuations during cycling, thus simultaneously improving ion transport efficiency and interfacial durability.[193,194] Suo *et al.* incorporated liquid metal (GalnSn) nanoparticles into a PEO matrix, creating a highly resilient PEO@LM composite with electric-field-driven self-healing functionality.[183] The liquid metal filler reduced PEO crystallinity *via* hydrogen bonding interactions, boosting ionic conductivity to 1.62×10^{-4} S cm^{-1} and expanding the electrochemical window to 5.2 V, which enabled self-healing at the electrolyte–anode interface through electric-field-induced migration (Fig. 6e). Metal–organic frameworks (MOFs) represent another promising class of inert fillers for CPEs, owing to their well-defined porosity, large surface area, abundant surface functional groups, and excellent thermal and chemical stability.[195] Tian *et al.* incorporated a 3D Cu-MOF into a PEO-based electrolyte, where open metal sites competitively coordinated with both $TFSI^-$ anions and ether oxygens in PEO, weakening the binding between Na^+ and the polymer chain.[196] This facilitated ion release and migration, leading to a room-

temperature conductivity of 1.03×1^{-4} S cm^{-1}, a cation transference number of 0.58, and effective suppression of dendritic plating.

4 Interface engineering

Interfacial challenges remain a critical bottleneck in advancing SSSBs.[197,198] The anode–electrolyte and cathode–electrolyte interfaces are two core components of SSSBs, both of which face common issues that restrict battery performance.[199,200] However, the two interfaces also have distinct problems due to differences in potential environments and material characteristics.[201,202]

4.1 Anode–electrolyte interface

For SSSBs, the anode/electrolyte interface is critical, primarily concerning the physical and chemical contact between sodium metal or alloy anodes and solid electrolytes, which must facilitate efficient ion conduction pathways. Achieving reversible sodium plating and stripping without dendrite formation remains a key challenge.[203,204] Research indicates that polymer-based electrolytes generally offer more stable and closer interfacial contact with sodium anodes compared to inorganic solid electrolytes, where dendritic growth is prevalent, which often leads to grain boundary penetration. Furthermore, repeated volume expansion and contraction of the sodium anode during cycling can degrade interfacial adhesion, resulting in poor long-term cycling stability.[205,206] Therefore, effective interfacial engineering between sodium anodes and inorganic solid electrolytes is essential to minimize interfacial resistance and improve overall battery performance.

4.1.1 SSE design. Due to their inherent brittleness, β-Al_2O_3 and NASICON-type electrolytes typically require high-temperature pressing techniques to achieve intimate interfacial contact. The interfacial contact of the metallic anode with the SSE significantly influences the cycling stability of SSSBs. In one case, the NASICON-type electrolyte has been modified through phase tuning to form $Na_{3.36}Zr_{1.64}Sc_{0.36}Si_2PO_{12}$ (NZSSP), synthesized *via* solid-state reactive sintering.[169] When sintered at 1150 °C, NZSSP exhibits a remarkably lower interfacial

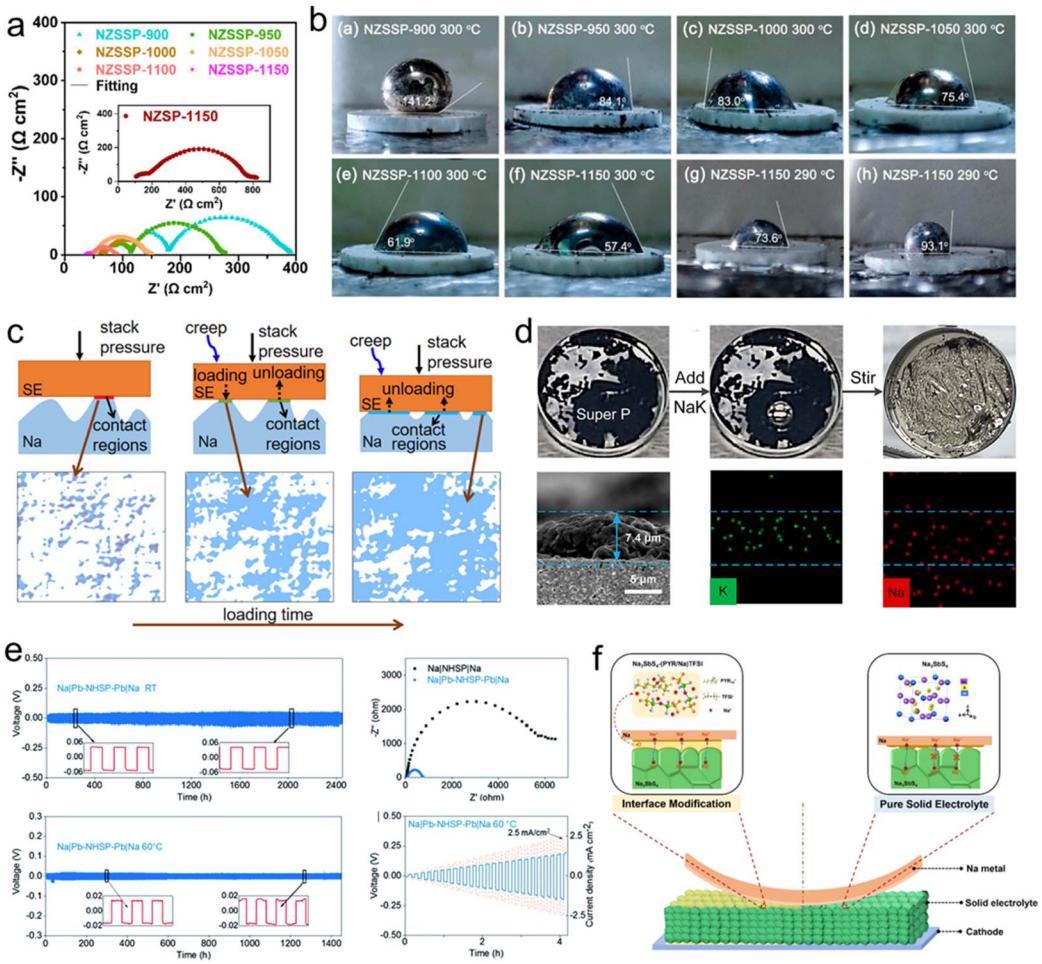

Fig. 7 (a) EIS spectra of Na/NZSSP/Na symmetrical cells. (b) Pictures of Na on different SSEs.[169] Copyright 2023, American Chemical Society. (c) Surface evolution with time due to creep.[209] Copyright 2021, American Chemical Society. (d) Fabrication and SEM images of the C@Na–K interface.[210] Copyright 2023, American Chemical Society. (e) The electrochemical performance of Pb decorated $Na_3Hf_2Si_2PO_{12}$.[211] Copyright 2022, The Royal Society of Chemistry. (f) Schematic diagram of the Na_3SbS_4/Na interface with the (PYR/Na)TFSI interlayer.[212] Copyright 2022, Elsevier.

impedance of 4.7 Ω cm^2 (Fig. 7a) and a higher critical current density of 0.85 mA cm^{-2} compared to the NZSP at 30 °C. Additionally, the rhombohedral phase of NASICON demonstrates stronger sodium adsorption energy and a reduced contact angle as shown in Fig. 7b, promoting better interfacial compatibility and facilitating smoother sodium deposition and dissolution processes. Applying external stack pressure during cell assembly has also been explored as a means to improve interfacial contact and reduce resistance at both anode and cathode interfaces. Kundu *et al.* investigated the effect of mechanical pressure on interfacial reactivity in sodium–SSE interfaces, reporting the development of a dense interphase in the Na–Na_3PS_4 system under moderate pressure.[207] However, continued growth of this ionically resistive layer leads to a steady rise in impedance over time. Moreover, after cold-pressing procedures, gaps often form between the sodium anode and electrolyte due to insufficient adhesion, negatively impacting electrochemical performance. In contrast, the Na/β-Al_2O_3 system exhibits superior interfacial stability with minimal parasitic reactions, highlighting its potential for stable sodium metal anode integration.[208] Wu *et al.* employed a 3D time-resolved model to detect the evolution of interfaces between sodium metal and Na-β″-Al_2O_3 SSE.[209] As presented in Fig. 7c, sodium metal achieved more favorable contact with the SSE than lithium, resulting in lower interfacial resistance.

4.1.2 Regulating interfacial wettability. Improving the interfacial wettability between the anode and SSE is a promising strategy to effectively lower interfacial impedance.[213] It has been proposed that using liquid sodium or sodium-based alloys like Na–K and Na–Ce can achieve excellent interfacial contact without the need for additional liquid additives. These sodium alloys remain in a liquid state at room temperature, which not only enhances interface compatibility but also inherently suppresses dendrite formation. Liu *et al.* developed a quasi-liquid alloy anode interface (C@Na–K) that exhibits both stability and dendrite-inhibiting characteristics for use in SSSBs, as shown in Fig. 7d.[210] Thanks to the superior wetting behaviour of the liquid phase between the anode and SSE, continuous physical contact is maintained, promoting efficient charge transfer and leading to enhanced electrochemical performance. Interfacial reactivity also plays a crucial role in determining wettability, with stronger chemical interactions generally improving wetting performance. Wang *et al.* investigated interfacial reactivity by coating NASICON-type $Na_3Hf_2Si_2PO_{12}$ (NHSP) electrolytes with various metals including Pb, Sn, Cu, and Cr to evaluate their impact on interfacial properties and charge transfer kinetics.[211] Among the metals, Pb demonstrated optimal results, forming an interphase with sodium that exhibited excellent wettability and rapid ion conduction. This contributed to enhanced interfacial stability, enabling the Pb-modified NHSP-based battery to operate stably for over 2400 hours at ambient temperature and achieve a critical current density of 2.5 mA cm^{-2} at 60 °C (Fig. 7e). Drawing inspiration from the favourable interfacial characteristics of liquid electrolytes, researchers have introduced organic liquids and ionic liquids (ILs) as wetting agents to improve contact between the anode and SSE. In one study, Wang's group proposed an effective interlayer by utilizing an IL electrolyte to stabilize the Na/SSE interface, as illustrated in Fig. 7f.[212] Owing to its high electrochemical stability and strong wetting ability, the FeS_2‖Na quasi-solid-state battery achieved a remarkable specific capacity exceeding 300 mAh g^{-1} at 20 mA g^{-1} and retained a capacity of 103 mAh g^{-1} after 330 cycles at 100 mA g^{-1}, demonstrating exceptional long-term cycling durability.

4.1.3 Introducing functional interlayers. Introducing an interlayer with high ionic conductivity, negligible electronic conduction, and excellent chemical compatibility with both the sodium anode and SSE at the anode–electrolyte interface can significantly improve interfacial characteristics.[214] Such a design helps minimize interfacial resistance and ensures robust physical contact. Huo *et al.* developed an integrated, sandwich-structured NZSP-based composite electrolyte by engineering artificial interfacial layers on both electrode sides.[215] A uniformly coated SbF_3 layer on the anode side of NZSP rapidly reacts during discharge to form a conductive layer containing Na_xSb and NaF, which effectively hinders dendritic sodium growth (Fig. 8a). Owing to this tailored interface architecture, symmetric cells achieved a critical current density of 1.9 mA cm^{-2} and exhibited exceptional cycling stability, sustaining uniform plating/stripping for over 2600 hours at current densities of 0.1 and 0.2 mA cm^{-2}, respectively. Chen's group introduced an innovative interfacial healing approach for SSSBs, leveraging an electro-triggered polymerization process accelerated by charged microdroplets and enhancing the polymerization rate by 21.4 times.[216] The strategy utilizes charge-driven electrowetting to enable rapid and uniform deposition of protective coatings at the interface, which not only extend air stability but also selectively infiltrate microcracks and voids, thereby reinforcing interfacial integrity, improving component compatibility, and preventing crack propagation induced by dendrite penetration. As a result, a remarkably high critical current density of 6.8 mA cm^{-2} was attained, and full cells demonstrated stable operation for more than 1000 cycles at 1.0C. Artificial SEI engineering has also proven effective in addressing interfacial instability. Qi *et al.* fabricated a poly(-methyl methacrylate) (poly(MMA))-based artificial SEI on commercial hard carbon anodes.[217] The engineered interface modifies the Na^+–DME solvation structure at the inner Helmholtz plane, transforming it into a coordinated environment involving Na^+–DME and poly(MMA) (Fig. 8b). This reconfiguration promotes efficient desolvation of Na^+ ions and accelerates interfacial ion transport, leading to outstanding rate capability (236 mAh g^{-1} at 5C) and exceptional long-term stability, with 99% capacity retention after 1000 cycles.

4.1.4 Developing sodium anode composites or alloys. Beyond interfacial modification strategies, fabricating sodium-based alloys or composite anodes represents another promising route to mitigate interfacial challenges.[220,221] One such composite anode was synthesized by melting a mixture of 5 wt% indium and 95 wt% sodium at 180 °C, resulting in a dispersed sodiophilic Na_2In phase.[218] As shown in Fig. 8c, this bulk reconstruction approach creates abundant sodiophilic sites both on the surface and within the bulk, effectively alleviating issues related to dendrite formation, interfacial delamination,

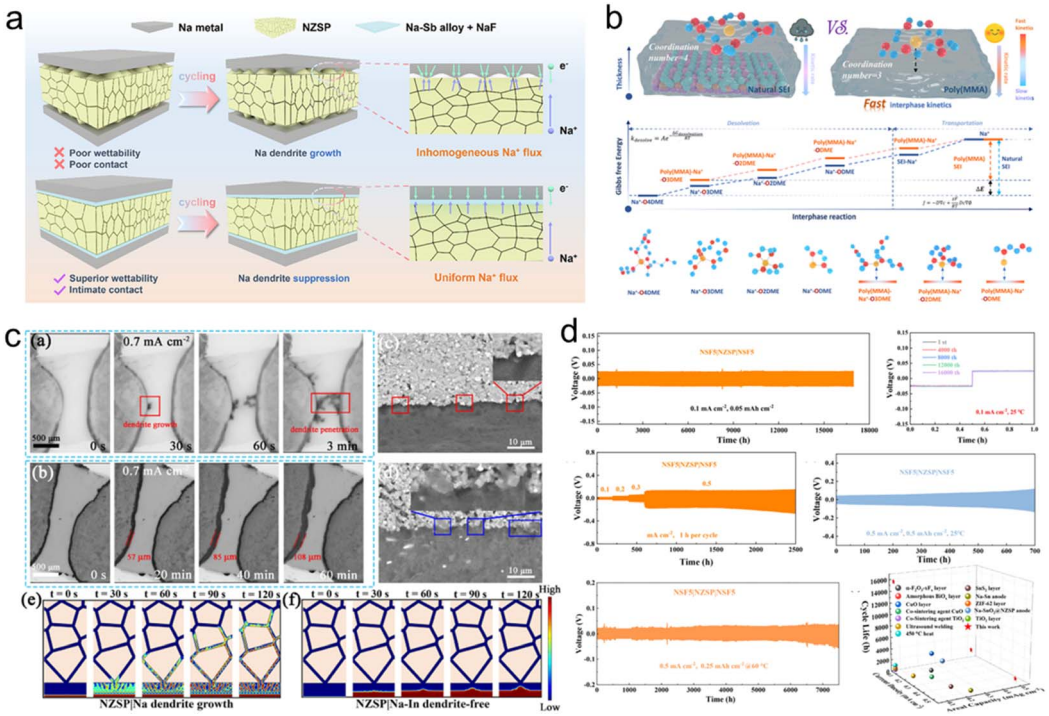

Fig. 8 (a) Schematic of the mechanism for Na plating/stripping at the Na/NZSP and Na/SbF_3-NZSP interface.[215] Copyright 2025, Wiley-VCH. (b) Schematic illustration of different coordination structures and desolvation energy barriers of Na^+ at the natural SEI and poly(MMA) interface.[217] Copyright 2025, Wiley-VCH. (c) Sodium deposition behavior of Na|NZSP|Na and Na–In|NZSP|Na–In at a current density of 0.7 mA cm^{-2}.[218] Copyright 2025, Wiley-VCH. (d) Electrochemical performance of an NZSP-based symmetrical cell.[219] Copyright 2024, American Chemical Society.

and localized current accumulation. When paired with the NZSP electrolyte, symmetric cells employing this modified anode operated stably for over 1000 hours at 0.3 mA cm^{-2}, vastly outperforming conventional sodium metal anodes, which typically fail within 10 hours under similar conditions (Fig. 8d). Furthermore, a highly stable gradient-structured composite anode was developed *via in situ* conversion and alloying reactions between SbF_3 and molten sodium.[219] This composite features a tightly bonded solid–solid interface with the sodium superionic conductor oxide electrolyte, enriched with NaF at the boundary and Na_3Sb within the bulk anode. The dual-phase architecture suppresses dendrite nucleation while facilitating rapid bulk-to-interface sodium ion transport. Leveraging these advantages, both symmetric and full battery configurations incorporating this composite anode exhibit superior electrochemical performance, highlighting the potential of compositional and structural engineering in next-generation sodium metal anodes.

4.2 Cathode–electrolyte interface

The physical contact between the cathode and SSE at the microscopic level typically remains limited to point-to-point interaction, resulting in elevated interfacial impedance and sluggish kinetics of sodium ion migration. Furthermore, repeated volume changes of cathodes during sodium ion insertion and extraction processes can induce mechanical separation at the cathode–electrolyte interface, exacerbating interfacial degradation.[222] This deterioration further increases resistance and accelerates capacity fading, ultimately reducing the cycle life of SSSBs. Besides, the cathode–electrolyte interface operates under high electrochemical potentials, creating favorable conditions for redox side reactions. These approaches aim to suppress undesirable side reactions at high voltages, accommodate volumetric strain during cycling, reduce interfacial resistance, prevent loss of ionic conductivity due to interface separation or insulating byproduct formation and thereby enhance overall cycling stability (Fig. 9a).[223]

4.2.1 Composites of electrolytes and cathodes. In conventional fabrication methods for SSSBs, the cathode and electrolyte are independently prepared and later assembled under high pressure. This approach results in only surface contact between the cathode and SSE, restricting ionic conduction pathways and limiting ion transport efficiency.[224] A widely adopted solution for both inorganic and organic solid electrolyte systems involves fabricating composite cathodes by uniformly mixing active materials with SSEs. For instance, bulk-type SSSBs have been successfully constructed by chemically infiltrating the precursor solution of the $Na_3V_2P_3O_{12}$ cathode into the framework of the $Na_{3.4}Zr_2Si_{2.4}P_{0.6}O_{12}$ electrolyte (Fig. 9b), which facilitated the formation of a well-integrated $Na_3V_2P_3O_{12}$ nanolayer on the $Na_{3.4}Zr_2Si_{2.4}P_{0.6}O_{12}$ skeleton, promoting efficient ion transport while mitigating mechanical stress arising from volume changes during repeated cycles.[225] As a result, stable electrochemical performance is achieved at

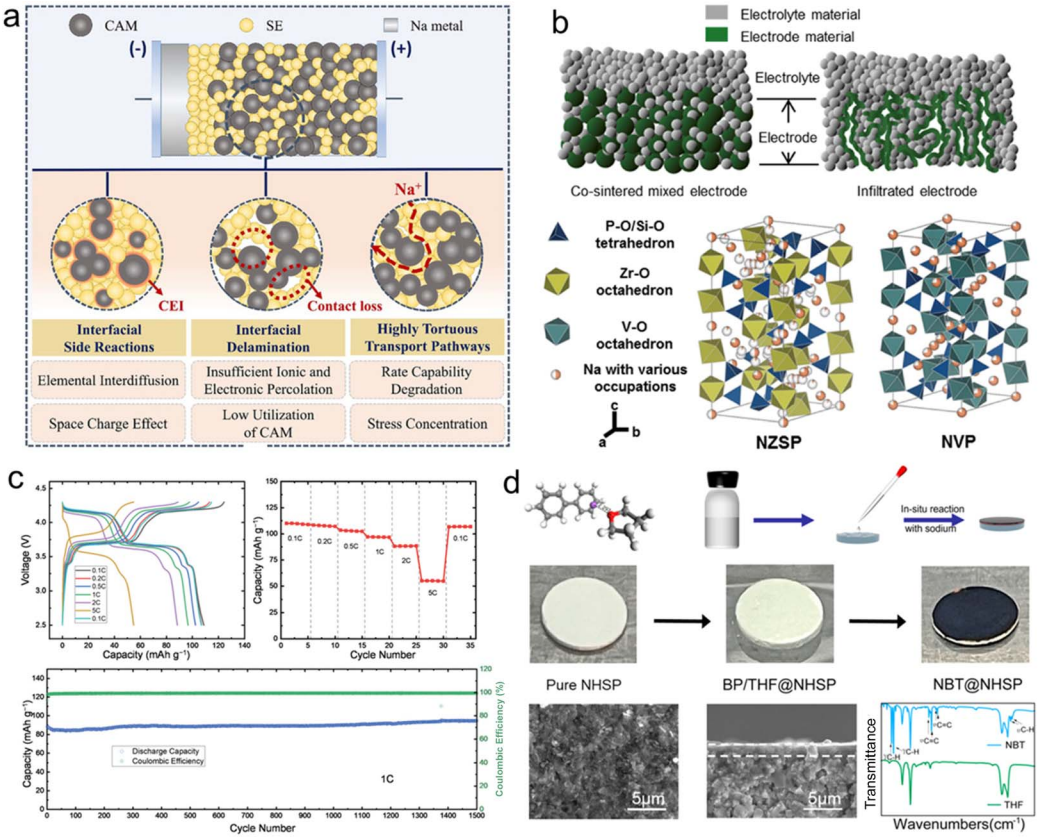

Fig. 9 (a) Interfacial issues between cathodes and SSEs.[223] Copyright 2025, Wiley-VCH. (b) Design and fabrication of chemically infiltrated SSSBs with the $Na_3V_2P_3O_{12}$ cathode and $Na_{3.4}Zr_2Si_{2.4}P_{0.6}O_{12}$ electrolyte.[225] Copyright 2019, Elsevier. (c) Electrochemical performance of NVPF in a hybrid SSE.[227] Copyright 2023, Wiley-VCH. (d) Construction of NBT on an SSE.[228] Copyright 2022, American Chemical Society.

room temperature. Despite such improvements, the contact remains largely physical and point-based, making it difficult to achieve optimal lattice matching necessary for fast Na^+ diffusion. Moreover, continuous expansion and contraction may still lead to interfacial separation over time, weakening ion conduction and degrading cycling behavior. Honma *et al.* demonstrated an alternative approach through pressure-less co-firing at 550 °C, integrating $Na_2FeP_2O_7$ crystallized glass with a β″-Al_2O_3 solid electrolyte.[226] During the crystallization process of the Na_2O–Fe_2O_3–P_2O_5 glass system, atomic-scale fusion with the β″-Al_2O_3 occurs, forming both physical and chemical bonds at the interface. This robust integration significantly lowers interfacial resistance and prevents separation, enabling the cell to maintain structural integrity over 623 cycles without performance decay.

4.2.2 Wetting agents on the interface. The inherent advantages of liquid electrolytes, particularly for their excellent wettability and high ionic mobility, make them superior to solid electrolytes in establishing intimate interfacial contact.[229] To leverage these properties, both organic liquid electrolytes and ILs have been employed as interfacial wetting agents to improve adhesion between the cathode and SSE, thereby facilitating faster sodium ion transport kinetics. However, conventional liquid electrolytes suffer from thermal instability, limiting their practical use. In contrast, ILs are favored due to their non-flammable nature, negligible vapor pressure, and outstanding thermal and electrochemical robustness. Hagiwara *et al.* developed a $Na[PF_6]$–$[DEME][PF_6]$ IL that exhibits exceptional oxidative stability up to 5.2 V on pT and over 4.5 V on conductive carbon, effectively preventing oxidative degradation of β-Al_2O_3 solid electrolytes while enhancing interfacial compatibility between the cathode and electrolyte.[227] This improvement extends the electrochemical stability window in hybrid solid electrolyte systems. Utilizing the β-Al_2O_3/IL electrolyte configuration, a hybrid SSSB incorporating the high-voltage cathode material $Na_3V_2(PO_4)_2F_3$ (NVPF) was successfully fabricated, demonstrating high energy density and excellent cycling durability, as displayed in Fig. 9c. Liu *et al.* constructed a fluidic interfacial layer (NBT) on a $Na_3Hf_2Si_2PO_{12}$ solid electrolyte through a facile *in situ* chemical reaction, as shown in Fig. 9d.[228] It possesses high fluidity and superior ionic conductivity, ensuring tight, homogeneous interfacial contact and enabling rapid and uniform sodium ion transport. This optimized interface significantly reduces interfacial resistance and effectively hinders the growth of sodium dendrites. Consequently, highly reversible sodium plating and stripping were achieved with minimal overpotential, even under a high current density of 0.5 mA cm^{-2}.

4.2.3 Interlayer/interphase between the cathode and electrolyte. It has been widely observed that when operating above 3.8 V, especially with oxide- or sulfide-based solid electrolytes, side electrochemical reactions occur at the cathode–electrolyte

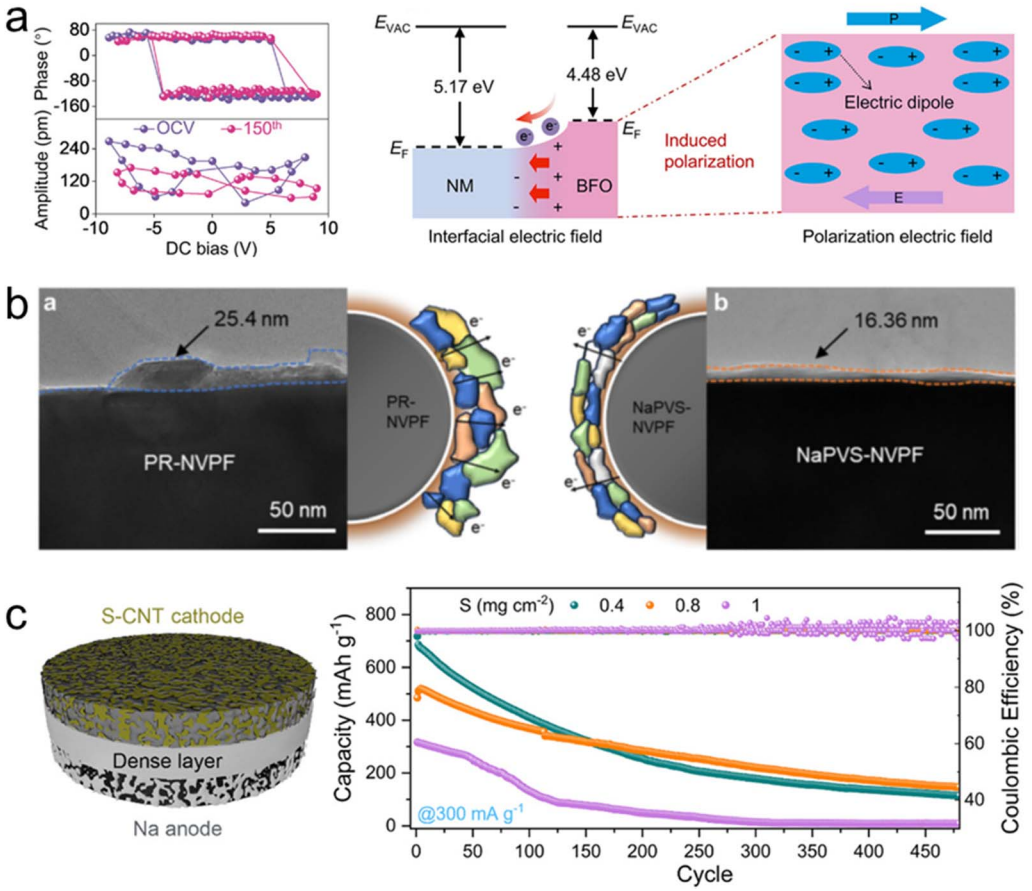

Fig. 10 (a) Analysis of the synergistic ferroelectric–magnetic effect on the cathode–electrolyte interface.[231] Copyright 2025, Wiley-VCH. (b) TEM images of pristine-NVPF and 5 wt% NaPVS-NVPF cathode particles after 50 cycles.[232] Copyright 2025, Springer Nature. (c) Electrochemical performance of the monolithic electrolyte.[234] Copyright 2021, American Chemical Society.

interface. These undesired reactions not only decompose the electrolyte but also restrict the use of high-voltage cathode materials.[230] To address this issue, inserting a functional interlayer or constructing a stable interphase between the cathode and SSE has emerged as a promising strategy to inhibit interfacial decomposition and lower charge transfer resistance. For instance, introducing a multiferroic $BiFeO_3$ (BFO) layer on the cathode surface activates a synergistic ferroelectric–magnetic effect at the $NaNi_{0.5}Mn_{0.5}O_2$-electrolyte interface (Fig. 10a), significantly boosting its fast-charging capability and long-term cycling stability.[231] First, the synergy regulated the nucleation and growth of the interfacial phase, promoting the formation of a thin and NaF-rich layer that enhanced interfacial ion transport. Second, the optimized layer ensured a uniform distribution of sodium ions across the interface, accelerating charge transfer kinetics. Third, the design alleviated local distortion within the NiO_6 octahedra, reducing structural strain during cycling and improving overall electrode integrity. Li's group introduced sodium polyvinyl sulfonate (NaPVS) as a multifunctional cathode additive to regulate the interface between the cathode and PEO-based electrolyte in SSSBs, as shown in Fig. 10b.[232] Strong ion–dipole interactions between the sulfonate groups in NaPVS and the cathode surface enabled homogeneous dispersion of the additive. During the initial electrochemical cycles, a cathode–electrolyte interphase composed of both organic and inorganic sulfur-containing compounds is *in situ* formed. This protective layer effectively prevents direct contact between the PEO electrolyte and the high-voltage cathode, thereby enhancing the oxidative stability of the polymer electrolyte under elevated potentials. Moreover, polyethylene glycol has also been explored as an additive in NASICON-type quasi-solid electrolytes.[233] The integration enhances the coordination environment between Na^+ ions and solvent molecules, which stabilizes the solvation structure while simultaneously reducing solvent evaporation, thereby leading to improved ionic conductivity and enhanced interfacial compatibility between the electrolyte and electrodes.

4.2.4 Structural design of the electrolyte and cathode. As previously discussed, composite electrolytes that combine the high ionic conductivity of inorganic ceramics with the flexibility of organic polymers have been developed to minimize interfacial resistance between solid electrolytes and electrodes. Besides, structural design of both the electrolyte and cathode has emerged as a powerful strategy for achieving close and durable interfacial contact. Wen *et al.* designed a β″-Al_2O_3 electrolyte featuring a vertically aligned porous–dense bilayer architecture to address key interfacial challenges.[235] The upper carbon-coated porous layer acts as a host for the high-loading

NVP material, enabling efficient electron and ion transport pathways. Meanwhile, the underlying dense layer serves as a mechanical barrier that inhibits sodium dendrite penetration and enhances the structural integrity of the electrolyte. As a consequence, this architecture enabled a cathode loading up to 8 mg cm^{-2}, while the resulting battery delivered a reversible specific capacity of 87 mAh g^{-1} and maintained 95.5% capacity retention over 100 cycles at 0.1C, which surpass those of conventional dense β″-Al_2O_3 electrolyte-based SSSBs. A monolithic multilayer electrolyte comprising two porous layers sandwiching a central dense layer was fabricated by substituting Zr^{4+} sites with Al^{3+} ions in a $Na_{3.4}Zr_2(Si_{0.8}P_{0.2}O_4)_3$ ceramic framework, effectively lowering interfacial resistance and suppressing dendrite formation.[234] Sulfur was introduced into one porous segment *via* vapor deposition, while molten sodium was infused into the opposite porous region, forming integrated electrode components. The unique design significantly reduces interfacial impedance and enables the development of high-performance solid-state sodium–sulfur batteries. The cell exhibited excellent cyclability, maintaining a discharge capacity of 300 mAh g^{-1} after 480 cycles at a current density of 300 mA g^{-1} (Fig. 10c), highlighting the effectiveness of architectural design in advancing solid-state battery technology.

5 Conclusions and outlook: from materials discovery to deployable solid-state sodium batteries

Despite substantial progress in the development of solid-state electrolytes for sodium batteries, the translation of promising materials properties into durable, high-performance full cells remains limited. This gap reflects not only unresolved materials challenges, but also a broader mismatch between laboratory-scale performance metrics and practical cell-level requirements. In particular, the widespread emphasis on achieving high bulk ionic conductivity has often obscured more critical factors, including interfacial resistance, mechanical integrity, critical current density, and long-term stability under realistic operating conditions.

Looking forward, it is instructive to distinguish between challenges that are fundamentally materials-limited and those that are predominantly engineering-limited. For polymer-based electrolytes, low room-temperature conductivity and insufficient oxidative stability remain intrinsic materials constraints, suggesting that their near-term deployment is most realistic in moderately elevated temperature regimes or hybrid configurations. In contrast, many inorganic electrolytes, including sulfides and NASICON-type ceramics, already exhibit adequate ionic conductivity, but suffer from severe interfacial and processing challenges, indicating that further progress will depend primarily on interface engineering, microstructural control, and scalable fabrication strategies rather than continued bulk material optimization.

β″-Al_2O_3-based electrolytes provide an instructive example of this distinction. Their long-standing success in high-temperature molten sodium batteries demonstrates that exceptional ionic conductivity and chemical stability can be achieved when materials properties are well matched with operating conditions. However, attempts to translate these advantages to lower-temperature solid-state configurations reveal that interfacial impedance, mechanical brittleness, and thermal mismatch rapidly become dominant limitations. These observations highlight that the viability of solid-state sodium batteries is inherently application-dependent, and that direct extrapolation from lithium-based solid-state paradigms may be neither necessary nor optimal.

From a technological perspective, the most realistic deployment pathways for solid-state sodium batteries in the next 5–10 years are likely to emerge in application spaces where sodium chemistry offers intrinsic advantages. These include large-scale stationary energy storage, high-temperature or thermally managed systems, and cost-sensitive applications that can tolerate moderate energy density in exchange for improved safety, durability, and resource sustainability. In such contexts, hybrid solid-state architectures, graded interfaces, and composite electrolytes that balance mechanical compliance with ionic transport may offer more immediate impact than fully inorganic, room-temperature sodium-metal configurations.

More broadly, sodium-based solid-state systems should not be viewed merely as lower-cost analogues of lithium solid-state batteries. Instead, their future competitiveness will depend on identifying operating regimes and cell designs that exploit the distinct electrochemical, mechanical, and thermodynamic characteristics of sodium. Achieving this goal will require a shift in research emphasis—from maximizing isolated materials metrics toward integrated cell-level design principles that explicitly couple ion transport, interfacial chemistry, and mechanical stability. By aligning materials development with realistic application targets, solid-state sodium batteries may ultimately establish technological niches that are complementary to, rather than directly competitive with, their lithium counterparts.

Author contributions

Mingyue Wang: conceptualization, writing – original draft, supervision, writing – review & editing. Qing Zhong: writing – original draft, writing – review & editing. Yue Wang & Xu Liu: formal analysis, investigation. Dongyang Zhang: investigation, supervision. Shujiang Ding: conceptualization, funding acquisition, supervision.

Conflicts of interest

There are no conflicts to declare.

Data availability

No primary research results, software or code have been included and no new data were generated or analyzed as part of this review.

Acknowledgements

This work is financially supported by the Key Projects of Shaanxi Province (2023GXLH-001), Xi'an Association for Science and Technology Young Talent Support Program Project (0959202513149) and Innovation Capability Support Plan of Shaanxi (no. 2022TD-27).

References

1 L. Miao, Z. Guo and L. Jiao, Insights into the design of mildly acidic aqueous electrolytes for improved stability of Zn anode performance in zinc-ion batteries, *Energy Mater.*, 2023, **3**, 300014.
2 G. Tang, Y. Li, J. Wu, Q. Kang and L. Ma, Engineering heterostructured electrocatalysts for enhanced sulfur redox kinetics in metal-sulfur batteries, *Nano Res. Energy*, 2025, **4**, e9120179.
3 J. Xu, Q. Kang, B. Peng, Z. Zhuang, D. Wang and L. Ma, Engineering single-atom catalysts for sulfur electrochemistry in metal–sulfur batteries, *J. Energy Chem.*, 2025, **106**, 768–790.
4 B. Zhu, W. Zhang, Z. Jiang, J. Chen, Z. Li, J. Zheng, N. Wen, R. Chen, H. Yang, W. Zong, Y. Dai, C. Ye, Q. Zhang, T. Qiu, Y. Lai, J. Li and Z. Zhang, Sodium compensation: a critical technology for transforming batteries from sodium-starved to sodium-rich systems, *Chem. Sci.*, 2024, **15**, 14104–14121.
5 Y. Zheng, L. Li, Y. Jiao, Y. Zhang, B. Peng, J. Xu and L. Ma, Recent advances in metal nitrides as highly-efficient electrocatalysts for lithium-sulfur batteries, *Nano Res.*, 2025, **18**, 94907542.
6 L. Ma, Q. Wu, M. He, J. Wu, B. Peng, J. Xu, J. Liu and Z. Jin, Binary Metal Alloy Electrocatalyst Synergistically Accelerates the Bidirectional Polysulfide Conversions in Lithium–Sulfur Batteries, *Nano Lett.*, 2025, **25**, 1939–1947.
7 L. Ma, G. Zhu, Z. Wang, A. Zhu, K. Wu, B. Peng, J. Xu, D. Wang and Z. Jin, Long-Lasting Zinc–Iodine Batteries with Ultrahigh Areal Capacity and Boosted Rate Capability Enabled by Nickel Single-Atom Electrocatalysts, *Nano Lett.*, 2023, **23**, 5272–5280.
8 M. Wang, Y. Wang, D. Zhang, X. Kong, Q. Rong, L. Zhou, J. Wang and S. Ding, Recent advances in emerging three-dimensional carbon-based architectures for ion transfer and storage in advanced metal-ion batteries, *J. Energy Storage*, 2025, **128**, 117173.
9 M. Wang, H. Zhang, J. Cui, S. Yao, X. Shen, T. J. Park and J.-K. Kim, Recent advances in emerging nonaqueous K-ion batteries: from mechanistic insights to practical applications, *Energy Storage Mater.*, 2021, **39**, 305–346.
10 Y. Li, Y. Mei, R. Momen, B. Song, Y. Huang, X. Zhong, H. Ding, W. Deng, G. Zou, H. Hou and X. Ji, Boosting the interfacial dynamics and thermodynamics in polyanion cathode by carbon dots for ultrafast-charging sodium ion batteries, *Chem. Sci.*, 2024, **15**, 349–363.
11 M. Wang, H. Zhao, Y. Wang, N. Li, X. Liu, D. Zhang, K. Xi and S. Ding, Melt-carbonization of liquid metal organic frameworks reconfigured hard carbon surface with boosted sodium storage, *Sci. China Chem.*, 2025, DOI: 10.1007/s11426-025-2880-y.
12 D. Ruan, Z. Cui, J. Fan, D. Wang, Y. Wu and X. Ren, Recent advances in electrolyte molecular design for alkali metal batteries, *Chem. Sci.*, 2024, **15**, 4238–4274.
13 Z. Xing, W. Zhao, B. Yu, Y. Wang, L. Zhou, P. Xiong, M. Chen and J. Zhu, Electrolyte Design Strategies for Aqueous Sodium-Ion Batteries: Progress and Prospects, *Small*, 2024, **20**, 2405442.
14 X. Ma, Y. Liu, Y. Zhang and Y. Gong, Layered sodium titanate with a matched lattice: a single ion conductor in a solid-state sodium metal battery, *Chem. Sci.*, 2023, **14**, 13812–13824.
15 T. Jin, X. Ji, P.-F. Wang, K. Zhu, J. Zhang, L. Cao, L. Chen, C. Cui, T. Deng, S. Liu, N. Piao, Y. Liu, C. Shen, K. Xie, L. Jiao and C. Wang, High-Energy Aqueous Sodium-Ion Batteries, *Angew. Chem., Int. Ed.*, 2021, **60**, 11943–11948.
16 H. Darjazi, M. Falco, F. Colò, L. Balducci, G. Piana, F. Bella, G. Meligrana, F. Nobili, G. A. Elia and C. Gerbaldi, Electrolytes for Sodium Ion Batteries: The Current Transition from Liquid to Solid and Hybrid systems, *Adv. Mater.*, 2024, **36**, 2313572.
17 C. Li, H. Xu, L. Ni, B. Qin, Y. Ma, H. Jiang, G. Xu, J. Zhao and G. Cui, Nonaqueous Liquid Electrolytes for Sodium-Ion Batteries: Fundamentals, Progress and Perspectives, *Adv. Energy Mater.*, 2023, **13**, 2301758.
18 J. Wu, Z. Song, Q. Huang, K. Zhu, D. Lin, X. Chen, X. Li, X. Chen, X. Li, L. Ma and Y. Chen, Electrolyte Engineering for Room-Temperature Sodium–Sulfur Batteries: Challenges, Strategies, and Future Perspectives, *Adv. Mater.*, 2026, **38**, e14290.
19 B. Jache and P. Adelhelm, Use of Graphite as a Highly Reversible Electrode with Superior Cycle Life for Sodium-Ion Batteries by Making Use of Co-Intercalation Phenomena, *Angew. Chem., Int. Ed.*, 2014, **53**, 10169–10173.
20 S. Tang, J. Li, Q. Yuan, C. Wang, T. Wang, W. Xiang, Y. Xiao, S. Xu and J. S. Yu, Anion screening in ether-based electrolytes for boosted sodium storage at low-temperature, *Energy Storage Mater.*, 2025, **81**, 104459.
21 X. Yu, R. Chen, L. Gan, H. Li and L. Chen, Battery Safety: From Lithium-Ion to Solid-State Batteries, *Engineering*, 2023, **21**, 9–14.
22 X. Yi, H. Fu, A. M. Rao, Y. Zhang, J. Zhou, C. Wang and B. Lu, Safe electrolyte for long-cycling alkali-ion batteries, *Nat. Sustain.*, 2024, **7**, 326–337.
23 X. Guo, Z. Xie, R. Wang, J. Luo, J. Chen, S. Guo, G. Tang, Y. Shi and W. Chen, Interface-Compatible Gel-Polymer Electrolyte Enabled by NaF-Solubility-Regulation toward All-Climate Solid-State Sodium Batteries, *Angew. Chem., Int. Ed.*, 2024, **63**, e202402245.
24 J. T. Kummer and N. Weber, Battery having a molten alkali metal anode and a molten sulfur cathode, *US Patent*, 3413150, 1968.
25 W. Hou, X. Guo, X. Shen, K. Amine, H. Yu and J. Lu, Solid electrolytes and interfaces in all-solid-state sodium

batteries: Progress and perspective, *Nano Energy*, 2018, **52**, 279–291.

26 H. Ahmad, K. T. Kubra, A. Butt, U. Nisar, F. J. Iftikhar and G. Ali, Recent progress, challenges, and perspectives in the development of solid-state electrolytes for sodium batteries, *J. Power Sources*, 2023, **581**, 233518.

27 B. Pandit, M. Johansen, B. P. Andersen, C. S. Martínez-Cisneros, B. Levenfeld, D. B. Ravnsbæk and A. Varez, All-solid-state sodium-ion batteries operating at room temperature based on NASICON-type NaTi2(PO4)3 cathode and ceramic NASICON solid electrolyte: A complete in situ synchrotron X-ray study, *Chem. Eng. J.*, 2023, **472**, 144509.

28 Y. Shuai, J. Lou, X. Pei, C. Su, X. Ye, L. Zhang, Y. Wang, Z. Xu, P. Gao, S. He, Z. Wang and K. Chen, Constructing an In Situ Polymer Electrolyte and a Na-Rich Artificial SEI Layer toward Practical Solid-State Na Metal Batteries, *ACS Appl. Mater. Interfaces*, 2022, **14**, 45382–45391.

29 Z. Yang, L. Chen, H. Jiang, X. Liang, J. Wei, Z. Xie, B. Tang and Z. Zhou, SnF2-Induced Highly Current-Tolerant Solid Electrolytes for Solid-State Sodium Batteries, *Adv. Funct. Mater.*, 2023, **33**, 2306558.

30 D. Li, C. Sun, C. Wang, J. Li, Z. Wang and H. Jin, Regulating Na/NASCION electrolyte interface chemistry for stable solid-state Na metal batteries at room temperature, *Energy Storage Mater.*, 2023, **54**, 403–409.

31 P. Zou, C. Wang, Y. He and H. L. Xin, Making Plasticized Polymer Electrolytes Stable Against Sodium Metal for High-Energy Solid-State Sodium Batteries, *Angew. Chem., Int. Ed.*, 2024, **63**, e202319427.

32 T. Liu, P. Xiang, Y. Li, Z. Li, H. Sun, J. Yang, Z. Tian and X. Yao, In Situ Forming Na–Sn Alloy/Na2S Interface Layer for Ultrastable Solid State Sodium Batteries, *Adv. Funct. Mater.*, 2024, **34**, 2316528.

33 Q. Wang, C. Yu, L. Li, X. Liu, X. Zhang, G. Gao, Y. Wang and G. Li, Sc-doping in Na3Zr2Si2PO12 electrolytes enables preeminent performance of solid-state sodium batteries in a wide temperature range, *Energy Storage Mater.*, 2023, **54**, 135–145.

34 J. Guo, F. Feng, S. Zhao, R. Wang, M. Yang, Z. Shi, Y. Ren, Z. Ma, S. Chen and T. Liu, Achieving Ultra-Stable All-Solid-State Sodium Metal Batteries with Anion-Trapping 3D Fiber Network Enhanced Polymer Electrolyte, *Small*, 2023, **19**, 2206740.

35 J. Huang, K. Wu, G. Xu, M. Wu, S. Dou and C. Wu, Recent progress and strategic perspectives of inorganic solid electrolytes: fundamentals, modifications, and applications in sodium metal batteries, *Chem. Soc. Rev.*, 2023, **52**, 4933–4995.

36 Y. Dong, P. Wen, H. Shi, Y. Yu and Z.-S. Wu, Solid-State Electrolytes for Sodium Metal Batteries: Recent Status and Future Opportunities, *Adv. Funct. Mater.*, 2024, **34**, 2213584.

37 Y. Zhu and Y. Mo, Materials Design Principles for Air-Stable Lithium/Sodium Solid Electrolytes, *Angew. Chem., Int. Ed.*, 2020, **59**, 17472–17476.

38 X. Feng, H. Fang, N. Wu, P. Liu, P. Jena, J. Nanda and D. Mitlin, Review of modification strategies in emerging inorganic solid-state electrolytes for lithium, sodium, and potassium batteries, *Joule*, 2022, **6**, 543–587.

39 M. Jin, S. Cheng, Z. Yang, Y. Luo and Y. Guo, A novel high-voltage solid electrolyte of Na3B24H23 for 4 V all-solid-state sodium battery, *Chem. Eng. J.*, 2023, **455**, 140904.

40 Y. Hu, J. Fu, J. Xu, J. Luo, F. Zhao, H. Su, Y. Liu, X. Lin, W. Li, J. T. Kim, X. Hao, X. Yao, Y. Sun, J. Ma, H. Ren, M. Yang, Y. Huang and X. Sun, Superionic amorphous $NaTaCl_6$ halide electrolyte for highly reversible all-solid-state Na-ion batteries, *Matter*, 2024, **7**, 1018–1034.

41 X. Lin, Y. Zhao, C. Wang, J. Luo, J. Fu, B. Xiao, Y. Gao, W. Li, S. Zhang, J. Xu, F. Yang, X. Hao, H. Duan, Y. Sun, J. Guo, Y. Huang and X. Sun, A Dual Anion Chemistry-Based Superionic Glass Enabling Long-Cycling All-Solid-State Sodium-Ion Batteries, *Angew. Chem., Int. Ed.*, 2024, **63**, e202314181.

42 V. Thangadurai and B. Chen, Solid Li- and Na-Ion Electrolytes for Next Generation Rechargeable Batteries, *Chem. Mater.*, 2022, **34**, 6637–6658.

43 C. Li, R. Li, K. Liu, R. Si, Z. Zhang and Y.-S. Hu, NaSICON: A promising solid electrolyte for solid-state sodium batteries, *Interdiscip. Mater.*, 2022, **1**, 396–416.

44 J. A. S. Oh, X. Xu, Z. Zeng, K. Wang, N. Y. J. Tan, E. Kok, J. Huang and L. Lu, Thin NASICON Electrolyte to Realize High Energy Density Solid-State Sodium Metal Battery, *Energy Environ. Mater.*, 2023, **6**, e12472.

45 C. Heubner, B. Matthey, T. Lein, F. Wolke, T. Liebmann, C. Lämmel, M. Schneider, M. Herrmann and A. Michaelis, Insights into the electrochemical Li/Na-exchange in layered LiCoO2 cathode material, *Energy Storage Mater.*, 2020, **27**, 377–386.

46 P. Yang, Z. Wu, Y. Liang, H. Chen, C. Lin, J. Qiu, J. Meng, Y. He and S. Zhang, Engineering ion transport in all-solid-state sodium-ion batteries: fundamentals, strategies, and perspectives, *Prog. Mater. Sci.*, 2025, **154**, 101503.

47 H. Chen, H. Zang, J. Du, H. Zhang, X. Xu, P. Zhang, X. Li, J. Han, X.-L. Li and Q.-C. Wang, Leveraging Lewis Acid–Modulated Polymer–Inorganic Interface for High–Performance Solid–State Sodium Batteries, *Adv. Funct. Mater.*, 2025, **35**, 2504177.

48 H. Li, J. Huang, Y. Wu, T. Wang, S. Wu, S. Li and T. Yan, Organic Electrolyte Composed of Strongly and Weakly Coordinating Molecules for Sodium-Ion Battery. A Molecular Dynamics Simulation Study, *Energy Environ. Mater.*, 2026, e70147.

49 T. Deng, X. Ji, L. Zou, O. Chiekezi, L. Cao, X. Fan, T. R. Adebisi, H.-J. Chang, H. Wang, B. Li, X. Li, C. Wang, D. Reed, J.-G. Zhang, V. L. Sprenkle, C. Wang and X. Lu, Interfacial-engineering-enabled practical low-temperature sodium metal battery, *Nat. Nanotechnol.*, 2022, **17**, 269–277.

50 R. Fang, Y. Li, N. Wu, B. Xu, Y. Liu, A. Manthiram and J. B. Goodenough, Ultra-Thin Single-Particle-Layer Sodium Beta-Alumina-Based Composite Polymer Electrolyte Membrane for Sodium-Metal Batteries, *Adv. Funct. Mater.*, 2023, **33**, 2211229.

51 Z. Lu, H. Yang, G. Wu, P. Shan, H. Lin, P. He, J. Zhao, Y. Yang and H. Zhou, A "Liquid-In-Solid" Electrolyte for

High-Voltage Anode-Free Rechargeable Sodium Batteries, *Adv. Mater.*, 2024, **36**, 2404569.
52 A. Nasu, T. Inaoka, F. Tsuji, K. Motohashi, A. Sakuda, M. Tatsumisago and A. Hayashi, Formation of Passivate Interphases by Na3BS3-Glass Solid Electrolytes in All-Solid-State Sodium-Metal Batteries, *ACS Appl. Mater. Interfaces*, 2022, **14**, 24480–24485.
53 P. Song, S. Chen, J. Guo, J. Wu, Q. Lu, H. Xie, Q. Wang and T. Liu, Electrostatic Regulation of Na+ Coordination Chemistry for High-Performance All-Solid-State Sodium Batteries, *Nano-Micro Lett.*, 2025, **18**, 72.
54 F. Chen, Y. Xie, Z. Yu, N. Li, Y. Qiao and X. Ding, Robust Janus-faced quasi-solid-state honeycomb-mimicking electrolytes for the fast transport and adequate supply of sodium ions, *Chem. Sci.*, 2026, DOI: 10.1039/D5SC08536E.
55 S. Miao, Y. You, Z. Wang, Y. Zhao, H. Fan, X. Ai, Y. Cao and Y. Fang, Non-flammable electrolytes for high-safety sodium-ion batteries, *Chem. Soc. Rev.*, 2025, **54**, 9289–9316.
56 X. Xu, Z. Ai, Z. Xiu, Y. Shao, Y. Wu and X. Hao, Enhancing sodium ionic conductivity: An interface bridging strategy for Na3Zr2Si2PO12 solid-state electrolyte, *J. Energy Storage*, 2025, **115**, 116046.
57 H. Kwak, J.-S. Kim, D. Han, J. S. Kim, J. Park, G. Kwon, S.-M. Bak, U. Heo, C. Park, H.-W. Lee, K.-W. Nam, D.-H. Seo and Y. S. Jung, Boosting the interfacial superionic conduction of halide solid electrolytes for all-solid-state batteries, *Nat. Commun.*, 2023, **14**, 2459.
58 W. Wang, W. Yuan, Z. Zhao, D. Zou, P. Zhang, Z. Shi, J. Weng and P. Zhou, Enhanced ionic conductivity of Cu-doped NASICON solid electrolyte for solid-state sodium batteries, *J. Electroanal. Chem.*, 2023, **937**, 117405.
59 G. Liu, J. Yang, J. Wu, Z. Peng and X. Yao, Inorganic Sodium Solid Electrolytes: Structure Design, Interface Engineering and Application, *Adv. Mater.*, 2024, **36**, 2311475.
60 D. Lee, A. Kumar Kakarla, S. Sun, P. Joohyun Kim and J. Choi, Inorganic Solid-State Electrolytes for Solid-State Sodium Batteries: Electrolyte Design and Interfacial Challenges, *Chemelectrochem*, 2025, **12**, e202400612.
61 Y. Yang, S. Yang, X. Xue, X. Zhang, Q. Li, Y. Yao, X. Rui, H. Pan and Y. Yu, Inorganic All-Solid-State Sodium Batteries: Electrolyte Designing and Interface Engineering, *Adv. Mater.*, 2024, **36**, 2308332.
62 M. Akbar, M. Kim, I. Moeez, A. H. Umar Bhatti, Y. H. Kim, J. Jeong, J.-Y. Kim, J.-H. Park, S. Yu and K. Y. Chung, Dendrite-free Sb-doped NASICON-type Na3Zr2Si2PO12 solid-electrolyte for stable solid-state sodium batteries, *Chem. Eng. J.*, 2025, **504**, 158860.
63 A. Tiwari, D. Meghnani, R. Mishra, R. K. Tiwari, A. Patel and R. K. Singh, Impact of sintering temperature and ascertaining hopping bottlenecks for ions in sodium superionic conducting electrolyte for sodium-ion batteries, *J. Power Sources*, 2023, **580**, 233365.
64 Z. Li, J. Chen, Q. Fang, J. Fu, Y. Ren, X. Wang and X. Guo, Modulating Electric Double Layers via Polymer Electric Dipole Effects to Enhance Stability in Quasi-Solid-State Sodium Metal Batteries, *Angew. Chem., Int. Ed.*, 2025, **64**, e202505509.
65 F. Cheng, J. Hu, W. Zhang, B. Guo, P. Yu, X. Sun and J. Peng, Reviving ether-based electrolytes for sodium-ion batteries, *Energy Environ. Sci.*, 2025, **18**, 6874–6898.
66 Z. Xue, D. He and X. Xie, Poly(ethylene oxide)-based electrolytes for lithium-ion batteries, *J. Mater. Chem. A*, 2015, **3**, 19218–19253.
67 M. Yahia, M. Enterría, C. Pozo-Gonzalo and N. Ortiz-Vitoriano, A New Quasi-Solid Polymer Electrolyte for Next-Generation Na–O2 Batteries: Unveiling the Potential of a Polyamide-Polyether System, *Adv. Sci.*, 2025, **12**, e04490.
68 T. Hou, D. Wang, B. Jiang, Y. Liu, J. Kong, Y. He, Y. Huang and H. Xu, Ion bridging enables high-voltage polyether electrolytes for quasi-solid-state batteries, *Nat. Commun.*, 2025, **16**, 962.
69 T. Famprikis, P. Canepa, J. A. Dawson, M. S. Islam and C. Masquelier, Fundamentals of inorganic solid-state electrolytes for batteries, *Nat. Mater.*, 2019, **18**, 1278–1291.
70 L. Chen, Y. Li, S.-P. Li, L.-Z. Fan, C.-W. Nan and J. B. Goodenough, PEO/garnet composite electrolytes for solid-state lithium batteries: From "ceramic-in-polymer" to "polymer-in-ceramic", *Nano Energy*, 2018, **46**, 176–184.
71 H. Wang, Y. Sun, Q. Liu, Z. Mei, L. Yang, L. Duan and H. Guo, An asymmetric bilayer polymer-ceramic solid electrolyte for high-performance sodium metal batteries, *J. Energy Chem.*, 2022, **74**, 18–25.
72 P. Liu, L. Miao, Z. Sun, X. Chen, Y. Si, Q. Wang and L. Jiao, Inorganic–Organic Hybrid Multifunctional Solid Electrolyte Interphase Layers for Dendrite-Free Sodium Metal Anodes, *Angew. Chem., Int. Ed.*, 2023, **62**, e202312413.
73 X. Zheng, C. Shi, Z. Li, Z. Zhang, L. Yang, Q. Fang and J. Tang, In-Situ formation Inorganic/Organic solid electrolyte interphase and sodium affinity sites for improved sodium metal anodes, *Chem. Eng. J.*, 2025, **506**, 159713.
74 Y. Lu, L. Li, Q. Zhang, Z. Niu and J. Chen, Electrolyte and Interface Engineering for Solid-State Sodium Batteries, *Joule*, 2018, **2**, 1747–1770.
75 J. Evans, C. A. Vincent and P. G. Bruce, Electrochemical measurement of transference numbers in polymer electrolytes, *Polymer*, 1987, **28**, 2324–2328.
76 C. Sun, J. Liu, Y. Gong, D. P. Wilkinson and J. Zhang, Recent advances in all-solid-state rechargeable lithium batteries, *Nano Energy*, 2017, **33**, 363–386.
77 Z.-H. Luo, Y.-F. Du, Z.-J. Jiang, D. Zhang, N.-L. Shen, J.-X. Guo, F. Jiang, X. Liu, X. Zhang, X.-G. Qi, X. Shen, Y. Ma, Y. Zhong, J. He, Y. Wu and X.-B. Cheng, High-Entropy Inorganic Solid Electrolyte Interphase Enables Thermally Safe Sodium-Ion Battery with Deep Sodium Storage, *ACS Nano*, 2025, **19**, 39946–39960.
78 S. Lou, F. Zhang, C. Fu, M. Chen, Y. Ma, G. Yin and J. Wang, Interface Issues and Challenges in All-Solid-State Batteries: Lithium, Sodium, and Beyond, *Adv. Mater.*, 2021, **33**, 2000721.
79 C. Delmas, D. Carlier and M. Guignard, The Layered Oxides in Lithium and Sodium-Ion Batteries: A Solid-State Chemistry Approach, *Adv. Energy Mater.*, 2021, **11**, 2001201.

80 Q. Zhou, J. Ma, S. Dong, X. Li and G. Cui, Intermolecular Chemistry in Solid Polymer Electrolytes for High-Energy-Density Lithium Batteries, *Adv. Mater.*, 2019, **31**, 1902029.
81 L. Xiang, X. Li, J. Xiao, L. Zhu and X. Zhan, Interface issues and challenges for NASICON-based solid-state sodium-metal batteries, *Adv. Powder Mater.*, 2024, **3**, 100181.
82 Y. Liu, H. Mao, R. Bai, S. Weng, Q. Zhang, X. Rong, X. Chen, C. Zhang, S. Han, F. Ding, X. Wang, Y. Lu, J. Zhao, F. Wei, L. Chen and Y.-S. Hu, Designing an isotropic epilayer for stable 4.2 V solid-state Na batteries, *Nat. Energy*, 2025, DOI: 10.1038/s41560-025-01857-y.
83 Y. Zhao, C. Wang, Y. Dai and H. Jin, Homogeneous Na+ transfer dynamic at Na/Na3Zr2Si2PO12 interface for all solid-state sodium metal batteries, *Nano Energy*, 2021, **88**, 106293.
84 Y. Lu, C.-Z. Zhao, H. Yuan, X.-B. Cheng, J.-Q. Huang and Q. Zhang, Critical Current Density in Solid-State Lithium Metal Batteries: Mechanism, Influences, and Strategies, *Adv. Funct. Mater.*, 2021, **31**, 2009925.
85 K. Takada, Progress and prospective of solid-state lithium batteries, *Acta Mater.*, 2013, **61**, 759–770.
86 A. Banerjee, X. Wang, C. Fang, E. A. Wu and Y. S. Meng, Interfaces and Interphases in All-Solid-State Batteries with Inorganic Solid Electrolytes, *Chem. Rev.*, 2020, **120**, 6878–6933.
87 S. Qu, T. Niu, X. Qiao, Y. Shen, G. Cai, X. Wang, Y. Wang, Z. Zhou, S. Zhang, Z. Zhang, G. Li, G. Cai and J. Sun, Dual Optimization of Electrolyte and Interface in Na-β″-Al2O3 via Ga3+ Doping for Advanced Solid-State Sodium Batteries, *Adv. Mater.*, 2025, **37**, e03562.
88 P. Wang, Y. Niu, K. Zhang, W. Hou, X. Yao and Y. Xu, Adapting Crystal Structure and Grain Boundaries through Sm3+ Doping in Na3Zr2Si2PO4 for Boosting Applicability in Sodium Solid-State Batteries, *ACS Appl. Mater. Interfaces*, 2024, **16**, 2877–2887.
89 X. Bai, Y. Meng, H. Chen, D. Zhou and L.-Z. Fan, Regulation of Carrier Transport at Grain Boundaries of Na3Zr2Si2PO12 Solid Electrolyte with Ionic Conductor Filler for Superior Solid-State Sodium Batteries, *Adv. Funct. Mater.*, 2025, e19793.
90 J. Liu, L. Pei and J. Li, Enhancing interfacial stability between NASICON-type solid-state electrolytes and lithium metal anode via mixed ionic-electronic conductive interlayer engineering, *Chem. Eng. J.*, 2025, **519**, 165208.
91 P. Hu, Y. Zhang, X. Chi, K. Kumar Rao, F. Hao, H. Dong, F. Guo, Y. Ren, L. C. Grabow and Y. Yao, Stabilizing the Interface between Sodium Metal Anode and Sulfide-Based Solid-State Electrolyte with an Electron-Blocking Interlayer, *ACS Appl. Mater. Interfaces*, 2019, **11**, 9672–9678.
92 F. Li, M. Hou, L. Zhao, D. Zhang, B. Yang and F. Liang, Electrolyte and interface engineering for solid-state sodium batteries, *Energy Storage Mater.*, 2024, **65**, 103181.
93 G. Du, S. Wang, Z. Tong, X. Ji, X. Wei, Q. Zha, T. Zhai and H. Li, Dual thermal-stimulated self-adhesive mixed-phase interface to enable ultra-long cycle life of solid-state sodium metal batteries, *Energy Environ. Sci.*, 2025, **18**, 3689–3698.
94 J. Hou, T. Zhu, G. Wang, R. Cheacharoen, W. Sun, X. Lei, Q. Yuan, D. Sun and J. Zhao, Composite electrolytes and interface designs for progressive solid-state sodium batteries, *Carbon Energy*, 2024, **6**, e628.
95 Z. L. Dong, Y. Gan, V. Martins, X. Wang, B. Fu, E. Jin, Y. Gao, Y. Hu, X. Lin, Y. Yuan, C. Turner, X. Pang, H. Abdolvand, Y. Huang, T.-K. Sham and Y. Zhao, Novel Sulfide-Chloride Solid-State Electrolytes with Tunable Anion Ratio for Highly Stable Solid-State Sodium-Ion Batteries, *Adv. Mater.*, 2025, **37**, 2503107.
96 C. Liu, S. Jia, T. Yang, J. Liu, X. Zhou, Z. Wang, H. Dong, Z. Shi, Y. Zhang and Z. Chen, Scalable and Ultrathin Dual Entangled Network Polymer Electrolytes for Safe Solid-State Sodium Batteries, *Angew. Chem., Int. Ed.*, 2025, **64**, e202505938.
97 C. Zhao, L. Liu, X. Qi, Y. Lu, F. Wu, J. Zhao, Y. Yu, Y.-S. Hu and L. Chen, Solid-State Sodium Batteries, *Adv. Energy Mater.*, 2018, **8**, 1703012.
98 A. Wang, Q. Zhang, W. Li, K. Zhang, C. Dong, Y. Wang, X. Xu, Y. Liu, Z. Ren, F. Shen, Z. Song and X. Han, Electrochemical–Mechanical Evolution of Dendrites and Cracks in Na3Zr2Si2PO12 Ceramic Solid Electrolytes, *Adv. Energy Mater.*, 2025, **15**, e02156.
99 W. Shan, J. Chen, X. Wei, B. V. R. Chowdari, X. Wu and Z. Wen, Enhancing the Dendritic Tolerance of NASICON-Based Electrolytes by Grain Boundary Engineering, *ACS Appl. Mater. Interfaces*, 2025, **17**, 56144–56152.
100 S. Yang, N. Li, E. Zhao, C. Wang, J. He, X. Xiao, D. Fang, Q. Ni, X. Han, X. Xue, L. Chen, N. Li, J. Li, T. Guo, Y. Su and H. Jin, Imaging dendrite growth in solid-state sodium batteries using fluorescence tomography technology, *Sci. Adv.*, 2024, **10**, eadr0676.
101 L. Geng, D. Xue, J. Yao, Q. Dai, H. Sun, D. Zhu, Z. Rong, R. Fang, X. Zhang, Y. Su, J. Yan, S. J. Harris, S. Ichikawa, L. Zhang, Y. Tang, S. Zhang and J. Huang, Morphodynamics of dendrite growth in alumina based all solid-state sodium metal batteries, *Energy Environ. Sci.*, 2023, **16**, 2658–2668.
102 S. Zhao, H. Che, S. Chen, H. Tao, J. Liao, X.-Z. Liao and Z.-F. Ma, Research progress on the solid electrolyte of solid-state sodium-ion batteries, *Electrochem. Energy Rev.*, 2024, **7**, 3.
103 C. Zhao, L. Liu, X. Qi, Y. Lu, F. Wu, J. Zhao, Y. Yu, Y. S. Hu and L. Chen, Solid-state sodium batteries, *Adv. Energy Mater.*, 2018, **8**, 1703012.
104 Z.-Y. Li, Z. Li, J.-L. Fu and X. Guo, Sodium-ion conducting polymer electrolytes, *Rare Met.*, 2023, **42**, 1–16.
105 Y. L. Ni'Mah, M.-Y. Cheng, J. H. Cheng, J. Rick and B.-J. Hwang, Solid-state polymer nanocomposite electrolyte of TiO2/PEO/NaClO4 for sodium ion batteries, *J. Power Sources*, 2015, **278**, 375–381.
106 H. Chen, H. Zang, J. Du, H. Zhang, X. Xu, P. Zhang, X. Li, J. Han, X. L. Li and Q. C. Wang, Leveraging Lewis Acid–Modulated Polymer–Inorganic Interface for High–Performance Solid–State Sodium Batteries, *Adv. Funct. Mater.*, 2025, 2504177.

107 B. Yi, Z. Wei, S. Yao, S. Zhao, Z. Gao, S. Savilov, G. Chen, Z. X. Shen and F. Du, Challenges and prospectives of sodium-containing solid-state electrolyte materials for rechargeable metal batteries, *Mater. Sci. Eng. R Rep.*, 2025, **163**, 100949.

108 J. Hou, T. Zhu, G. Wang, R. Cheacharoen, W. Sun, X. Lei, Q. Yuan, D. Sun and J. Zhao, Composite electrolytes and interface designs for progressive solid-state sodium batteries, *Carbon Energy*, 2024, **6**, e628.

109 S. Wang, X. Lu, T. Zhang, Y. Kang, Y. Shi, Y. Tian, Z. Chen, H. Wang, Q. Ji and W. Huang, Nonflammable Polyfluorides-Anchored Quasi-Solid Electrolytes by Chemical-Crosslinking for High-Safety Sodium Metal Battery, *Adv. Funct. Mater.*, 2025, 2507147.

110 J. Yang, H. Zhang, Q. Zhou, H. Qu, T. Dong, M. Zhang, B. Tang, J. Zhang and G. Cui, Safety-enhanced polymer electrolytes for sodium batteries: recent progress and perspectives, *ACS Appl. Mater. Interfaces*, 2019, **11**, 17109–17127.

111 X. Wang, C. Zhang, M. Sawczyk, J. Sun, Q. Yuan, F. Chen, T. C. Mendes, P. C. Howlett, C. Fu and Y. Wang, Ultra-stable all-solid-state sodium metal batteries enabled by perfluoropolyether-based electrolytes, *Nat. Mater.*, 2022, **21**, 1057–1065.

112 X. Dong, X. Liu, H. Li, S. Passerini and D. Bresser, Single-ion conducting polymer electrolyte for superior sodium-metal batteries, *Angew. Chem.*, 2023, **135**, e202308699.

113 X. Dong, Y. Zhang, Z. You, Y. Chen, X. Wu and Z. Wen, Polyanion-Induced Single Na-Ion Polymer Electrolytes for Ultra-Stable Sodium Metal Batteries, *Adv. Funct. Mater.*, 2024, **34**, 2405931.

114 Y. Zhong, Y. Wang, L. Ma, P. He, J. Fang and J. Li, Endogenous triboelectricity enhancing the piezoelectric performance of fluorinated polyimide foam for sound detection, *Nano Energy*, 2025, **141**, 111129.

115 G. Feuillade and P. Perche, Ion-conductive macromolecular gels and membranes for solid lithium cells, *J. Appl. Electrochem.*, 1975, **5**, 63–69.

116 S. Wang, Y. Jiang and X. Hu, Ionogel-based membranes for safe lithium/sodium batteries, *Adv. Mater.*, 2022, **34**, 2200945.

117 M. Menisha, S. Senavirathna, K. Vignarooban, N. Iqbal, H. Pitawala and A. Kannan, Synthesis, electrochemical and optical studies of poly (ethylene oxide) based gel-polymer electrolytes for sodium-ion secondary batteries, *Solid State Ionics*, 2021, **371**, 115755.

118 M. L. Lehmann, G. Yang, J. Nanda and T. Saito, Well-designed crosslinked polymer electrolyte enables high ionic conductivity and enhanced salt solvation, *J. Electrochem. Soc.*, 2020, **167**, 070539.

119 S. Janakiraman, A. Surendran, R. Biswal, S. Ghosh, S. Anandhan and A. Venimadhav, Electrospun electroactive polyvinylidene fluoride-based fibrous polymer electrolyte for sodium ion batteries, *Mater. Res. Express*, 2019, **6**, 086318.

120 Y. Zhong, L. Ma, P. He, Q. Zhao and J. Li, Hybrid Piezo/Triboelectric Nanogenerators Based on Nanofibrous Aerogels for Energy Harvesting and Respiratory Monitoring, *ACS Sens.*, 2025, **10**, 8839–8851.

121 J. Zheng, W. Li, X. Liu, J. Zhang, X. Feng and W. Chen, Progress in gel polymer electrolytes for sodium-ion batteries, *Energy Environ. Mater.*, 2023, **6**, e12422.

122 H. Yang, Y. Chen, W. Tian, S. Yuan, P. Liu, Q. Wang, T. Jin and L. Jiao, Co-sustained Release Strategy of Nonflammable Gel Polymer Electrolytes Enables Long-Life Sodium Metal Batteries, *Angew. Chem., Int. Ed.*, 2025, e202506349.

123 W. Liang, K. Zhao, L. Ouyang, M. Zhu and J. Liu, A review of functional group selection and design strategies for gel polymer electrolytes for metal batteries, *Mater. Sci. Eng. R Rep.*, 2025, **164**, 100973.

124 S. Zhao, Y. Shen, H. Che, M. Jabeen, C. Lu, X. Z. Liao and Z. F. Ma, Cellulose Derivative and Polyionic Liquid Crosslinked Network Gel Electrolytes for Sodium Metal Quasi-Solid-State Batteries, *Adv. Funct. Mater.*, 2025, **35**, 2422162.

125 Y. Xu, D. Chen, L. Zheng, H. Fu, X. Ye, Y. Zhang, Z. Chen, Y. Zhong, X. Wang and J. Tu, Ester-ether Synergistic Interactions Regulating the Solvation Structure of Gel Polymer Electrolytes Enables Stable Sodium Metal Batteries, *Energy Storage Mater.*, 2025, 104533.

126 S. Zhao, Y. Shen, H. Che, X.-Z. Liao, X.-M. Zhang and Z.-F. Ma, Ionic conductive membrane suitable for sodium metal batteries, *J. Membr. Sci.*, 2024, **702**, 122792.

127 M. Akbar, I. Moeez, A. H. U. Bhatti, Y. H. Kim, M. Kim, J.-Y. Kim, J. Jeong, J. H. Park and K. Y. Chung, Antimony-doped NASICON-type solid electrolyte with homogeneous sodium-ion flux for high-temperature solid-state sodium batteries, *Chem. Eng. J.*, 2025, 164300.

128 G. Rankin and H. Merwin, The Ternary System CaO-Al2O3-MgO, *J. Am. Chem. Soc.*, 1916, **38**, 568–588.

129 X. Lu, G. Xia, J. P. Lemmon and Z. Yang, Advanced materials for sodium-beta alumina batteries: Status, challenges and perspectives, *J. Power Sources*, 2010, **195**, 2431–2442.

130 X.-S. Li, J. Liang, X. Cao, S.-Y. Zhu, Y.-F. Bai, J.-W. Sun, H.-B. Luo and J. Kong, Research progress of inorganic solid electrolyte materials for all-solid-state sodium-ion batteries, *Rare Met.*, 2025, **44**, 2871–2899.

131 Y. Yang, S. Yang, X. Xue, X. Zhang, Q. Li, Y. Yao, X. Rui, H. Pan and Y. Yu, Inorganic all-solid-state sodium batteries: electrolyte designing and interface engineering, *Adv. Mater.*, 2024, **36**, 2308332.

132 A. V. Virkar and R. S. Gordon, Fracture Properties of Polycrystalline Lithia-Stabilized β "-Alumina, *J. Am. Ceram. Soc.*, 1977, **60**, 58–61.

133 A. P. de Kroon, G. W. Schaefer and F. Aldinger, Direct Synthesis of Binary K-. beta.-and K-. beta.''-Alumina. 1. Phase Relations and Influence of Precursor Chemistry, *Chem. Mater.*, 1995, **7**, 878–887.

134 Z. Wang, X. Feng, T. Zhang, Z. Xie, F. Song and Y. Li, Preparation and characterization of CoO-doped and Li2O-stabilized Na-β″-Al2O3 solid electrolyte via a solid-state reaction method, *Ceram. Int.*, 2020, **46**, 24668–24673.

135 G. Chen, J. Lu, X. Zhou, L. Chen and X. Jiang, Solid-state synthesis of high performance Na-β″-Al2O3 solid electrolyte doped with MgO, *Ceram. Int.*, 2016, **42**, 16055–16062.

136 D. Xu, H. Jiang, Y. Li, L. Li, M. Li and O. Hai, The mechanical and electrical properties of Nb2 O5 doped Na-β″-Al2O3 solid electrolyte, *Eur. Phys. J. Appl. Phys.*, 2016, **74**, 10901.

137 S.-T. Lee, D.-H. Lee, J.-S. Kim and S.-K. Lim, Influence of Fe and Ti addition on properties of Na+-β/β″-alumina solid electrolytes, *Met. Mater. Int.*, 2017, **23**, 246–253.

138 G. Chen, J. Lu, L. Li, L. Chen and X. Jiang, Microstructure control and properties of β″-Al2O3 solid electrolyte, *J. Alloys Compd.*, 2016, **673**, 295–301.

139 H. Li, X. Jiang, J. Zhang and J. Zhang, Effect of excess Na2O on the sintering behavior and properties of sodium beta-alumina solid electrolyte, *Mater. Today Commun.*, 2023, **34**, 105203.

140 K. Zhao, Y. Liu, S. Zeng, J. Yang, Y. Liu, Z. Zhan and L. Song, Preparation and characterization of a ZrO2–TiO2-co-doped Na-β′′-Al2O3 ceramic thin film, *Ceram. Int.*, 2016, **42**, 8990–8996.

141 H. Chen, T. Wang, Z. Wang, A. Li, S. Cen, Z. Mao, J. Chen, X. Wang and C. Dong, Unlocking Solid-State Sodium–Metal Batteries at −15 °C by Electrolyte Optimization and Interface Regulation, *ACS Appl. Mater. Interfaces*, 2024, **17**, 1119–1126.

142 L. Ghadbeigi, A. Szendrei, P. Moreno, T. D. Sparks and A. V. Virkar, Synthesis of iron-doped Na-β″-alumina+ yttria-stabilized zirconia composite electrolytes by a vapor phase process, *Solid State Ionics*, 2016, **290**, 77–82.

143 S.-J. Shan, L.-P. Yang, X.-M. Liu, X.-L. Wei, H. Yang and X.-D. Shen, Preparation and characterization of TiO2 doped and MgO stabilized Na–β″-Al2O3 electrolyte via a citrate sol–gel method, *J. Alloys Compd.*, 2013, **563**, 176–179.

144 D.-H. Lee, S.-T. Lee, J.-S. Kim and S.-K. Lim, Analysis of properties of partially stabilized zirconia-doped Na+-beta-alumina prepared by calcining-cum-sintering process, *Mater. Res. Bull.*, 2017, **96**, 143–148.

145 D. Butts, J. R. Schoiber, C. Choi, G. N. J. Redhammer, N. Hüsing, S. Donne and B. Dunn, Fe-Substituted Sodium β″-Al2O3 as a High-Rate Na-Ion Electrode, *Chem. Mater.*, 2021, **33**, 6136–6145.

146 S.-T. Lee, D.-H. Lee, S.-M. Lee, S.-S. Han, S.-H. Lee and S.-K. Lim, Effects of calcium impurity on phase relationship, ionic conductivity and microstructure of Na+-β/β″-alumina solid electrolyte, *Bull. Mater. Sci.*, 2016, **39**, 729–735.

147 G. Zhang, Z. Wen, X. Wu, J. Zhang, G. Ma and J. Jin, Sol–gel synthesis of Mg2+ stabilized Na-β″/β-Al2O3 solid electrolyte for sodium anode battery, *J. Alloys Compd.*, 2014, **613**, 80–86.

148 C. Zhu and J. Xue, Structure and properties relationships of beta-Al2O3 electrolyte materials, *J. Alloys Compd.*, 2012, **517**, 182–185.

149 J. Lin, Z. Wen, X. Wang, S. Song and Y. Liu, Mechanochemical synthesis of Na-β/β″-Al2O3, *J. Solid State Electrochem.*, 2010, **14**, 1821–1827.

150 J. Wang, X.-P. Jiang, X.-L. Wei, H. Yang and X.-D. Shen, Synthesis of Na-β″-Al2O3 electrolytes by microwave sintering precursors derived from the sol–gel method, *J. Alloys Compd.*, 2010, **497**, 295–299.

151 S. C. Ligon, G. Blugan, M.-C. Bay, C. Battaglia, M. V. Heinz and T. Graule, Performance analysis of Na-β″-Al2O3/YSZ solid electrolytes produced by conventional sintering and by vapor conversion of α-Al2O3/YSZ, *Solid State Ionics*, 2020, **345**, 115169.

152 D. Li, X. Wang, Q. Guo, X. Yu, S. Cen, H. Ma, J. Chen, D. Wang, Z. Mao and C. Dong, Atomically bonding Na anodes with metallized ceramic electrolytes by ultrasound welding for high-energy/power solid-state sodium metal batteries, *Carbon Energy*, 2023, **5**, e299.

153 K. Li, Y. Yang, X. Zhang and S. Liang, Highly oriented β″-alumina ceramics with excellent ionic conductivity and mechanical performance obtained by spark plasma sintering technique, *J. Mater. Sci.*, 2020, **55**, 8435–8443.

154 K. Koganei, T. Oyama, M. Inada, N. Enomoto and K. Hayashi, C-axis oriented β″-alumina ceramics with anisotropic ionic conductivity prepared by spark plasma sintering, *Solid State Ionics*, 2014, **267**, 22–26.

155 D. Xu, H. Jiang, M. Li, O. Hai and Y. Zhang, Synthesis and characterization of Y2O3 doped Na–β″-Al2O3 solid electrolyte by double zeta process, *Ceram. Int.*, 2015, **41**, 5355–5361.

156 R. Li, D. Jiang, P. Du, C. Yuan, X. Cui, Q. Tang, J. Zheng, Y. Li, K. Lu, X. Ren, S. Gao and X. Zhan, Negating Na‖Na3Zr2Si2PO12 interfacial resistance for dendrite-free and "Na-less" solid-state batteries, *Chem. Sci.*, 2022, **13**, 14132–14140.

157 C. Lou, W. Zhang, J. Liu, Y. Gao, X. Sun, J. Fu, Y. Shi, L. Xu, H. Luo, Y. Chen, X. Gao, X. Kuang, L. Su and M. Tang, The glass phase in the grain boundary of Na3Zr2Si2PO12, created by gallium modulation, *Chem. Sci.*, 2024, **15**, 3988–3995.

158 A. K. Dey, S. S. Selvasundarasekar, S. Kundu, A. K. Mandal, A. Das and S. K. Pramanik, 2D organic nanosheets of self-assembled guanidinium derivative for efficient single sodium-ion conduction: rationalizing morphology editing and ion conduction, *Chem. Sci.*, 2024, **15**, 16321–16330.

159 K. B. Hueso, M. Armand and T. Rojo, High temperature sodium batteries: status, challenges and future trends, *Energy Environ. Sci.*, 2013, **6**, 734–749.

160 C. Bao, B. Wang, P. Liu, H. Wu, Y. Zhou, D. Wang, H. Liu and S. Dou, Solid electrolyte interphases on sodium metal anodes, *Adv. Funct. Mater.*, 2020, **30**, 2004891.

161 Z. Gao, Y. Bai, J. Feng, J. Yang, P. Liu, H. Yuan, X. Guan, F. R. Wang and Y. Huang, Controlling sodium dendrite growth via grain boundaries in Na3Zr2Si2PO12 electrolyte, *Adv. Energy Mater.*, 2024, **14**, 2304488.

162 Y. Li, M. Li, Z. Sun, Q. Ni, H. Jin and Y. Zhao, Recent advance on NASICON electrolyte in solid-state sodium metal batteries, *Energy Storage Mater.*, 2023, **56**, 582–599.

163 Y. Shao, G. Zhong, Y. Lu, L. Liu, C. Zhao, Q. Zhang, Y.-S. Hu, Y. Yang and L. Chen, A novel NASICON-based glass-ceramic

composite electrolyte with enhanced Na-ion conductivity, *Energy Storage Mater.*, 2019, **23**, 514–521.

164 Y. Li, C. Sun, Z. Sun, M. Li, H. Jin and Y. Zhao, Boosting Na-O Affinity in Na3Zr2Si2PO12 Electrolyte Promises Highly Rechargeable Solid-State Sodium Batteries, *Adv. Funct. Mater.*, 2024, **34**, 2403937.

165 B. Wei, S. Huang, X. Wang, M. Liu, C. Huang, R. Liu and H. Jin, Intermediate phase induced in situ self-reconstruction of amorphous NASICON for long-life solid-state sodium metal batteries, *Energy Environ. Sci.*, 2025, **18**, 831–840.

166 B. Xun, J. Wang, Y. Sato, S. Jia, S. Ohno, H. Akamatsu and K. Hayashi, Bifunctional Al dopant for enhancing bulk and grain boundary conductivities in sodium ion conducting NASICON ceramics, *Adv. Energy Mater.*, 2025, **15**, 2402891.

167 S. Liu, C. Zhou, Y. Wang, W. Wang, Y. Pei, J. Kieffer and R. M. Laine, Ce-substituted nanograin Na3Zr2Si2PO12 prepared by LF-FSP as sodium-ion conductors, *ACS Appl. Mater. Interfaces*, 2019, **12**, 3502–3509.

168 D. Zuo, L. Yang, Z. Zou, S. Li, Y. Feng, S. J. Harris, S. Shi and J. Wan, Ultrafast synthesis of NASICON solid electrolytes for sodium-metal batteries, *Adv. Energy Mater.*, 2023, **13**, 2301540.

169 H. Liu, Y. Xing, N. Chen, J. Wu, Y. Li and C. Zhang, Engineering the NASICON Electrolyte/Na Anode Interface by Tuning the Phase of Electrolyte for Solid-State Sodium Battery, *Chem. Mater.*, 2023, **35**, 8686–8694.

170 M. Akbar, M. Kim, I. Moeez, A. H. U. Bhatti, Y. H. Kim, J. Jeong, J.-Y. Kim, J.-H. Park, S. Yu and K. Y. Chung, Dendrite-free Sb-doped NASICON-type Na3Zr2Si2PO12 solid-electrolyte for stable solid-state sodium batteries, *Chem. Eng. J.*, 2025, **504**, 158860.

171 H. Nguyen, A. Banerjee, X. Wang, D. Tan, E. A. Wu, J.-M. Doux, R. Stephens, G. Verbist and Y. S. Meng, Single-step synthesis of highly conductive Na3PS4 solid electrolyte for sodium all solid-state batteries, *J. Power Sources*, 2019, **435**, 126623.

172 L. Zhang, D. Zhang, K. Yang, X. Yan, L. Wang, J. Mi, B. Xu and Y. Li, Vacancy-contained tetragonal Na3SbS4 superionic conductor, *Adv. Sci.*, 2016, **3**, 1600089.

173 Z. Zhang, E. Ramos, F. Lalère, A. Assoud, K. Kaup, P. Hartman and L. F. Nazar, Na 11 Sn 2 PS 12: a new solid state sodium superionic conductor, *Energy Environ. Sci.*, 2018, **11**, 87–93.

174 A. Hayashi, K. Noi, A. Sakuda and M. Tatsumisago, Superionic glass-ceramic electrolytes for room-temperature rechargeable sodium batteries, *Nat. Commun.*, 2012, **3**, 856.

175 Z. L. Dong, Y. Yuan, V. Martins, E. Jin, Y. Gan, X. Lin, Y. Gao, X. Hao, Y. Guan and J. Fu, Structural insight and modulating of sulfide-based solid-state electrolyte for high-performance solid-state sodium sulfur batteries, *Nano Energy*, 2024, **128**, 109871.

176 A. Nasu, T. Otono, T. Takayanagi, M. Deguchi, A. Sakuda, M. Tatsumisago and A. Hayashi, Utilizing reactive polysulfides flux Na2Sx for the synthesis of sulfide solid electrolytes for all-solid-state sodium batteries, *Energy Storage Mater.*, 2024, **67**, 103307.

177 A. Hayashi, N. Masuzawa, S. Yubuchi, F. Tsuji, C. Hotehama, A. Sakuda and M. Tatsumisago, A sodium-ion sulfide solid electrolyte with unprecedented conductivity at room temperature, *Nat. Commun.*, 2019, **10**, 5266.

178 J. Königsreiter, B. Gadermaier and H. M. R. Wilkening, Unveiling Ultra-High Ionic Conductivity in W-Doped Na3SbS4: Grain Boundary Effects and Pure Bulk Transport, *J. Am. Chem. Soc.*, 2025, **174**, 20092–20097.

179 Y. Guo, K. Liu, C. Li, D. Song, H. Zhang, Z. Wang, Y. Yan, L. Zhang and S. Dai, A Sulfide-Based Solid Electrolyte With High Humid Air Tolerance for Long Lifespan All-Solid-State Sodium Batteries, *Adv. Energy Mater.*, 2024, **14**, 2401504.

180 Z. L. Dong, Y. Gan, V. Martins, X. Wang, B. Fu, E. Jin, Y. Gao, Y. Hu, X. Lin and Y. Yuan, Novel Sulfide-Chloride Solid-State Electrolytes with Tunable Anion Ratio for Highly Stable Solid-State Sodium-Ion Batteries, *Adv. Mater.*, 2025, 2503107.

181 X. Wang, S. Zhang, J. Yue, X. Wang, Y. Xu, Y. Gong, L. Zhou, C. Zhao, J. Liang and X. Zhu, A New Class of Carbonate-Oxychloride Solid Electrolytes for High-Performance Sodium-Ion All-Solid-State Batteries, *Energy Environ. Sci.*, 2025, **18**, 9927–9938.

182 T. Wang, M. Zhang, K. Zhou, H. Wang, A. Shao, L. Hou, Z. Wang, X. Tang, M. Bai and S. Li, A hetero-layered, mechanically reinforced, ultra-lightweight composite polymer electrolyte for wide-temperature-range, solid-state sodium batteries, *Adv. Funct. Mater.*, 2023, **33**, 2215117.

183 J. Suo, Y. Jia, X. Zhu, S. Liu, X. Tang, F. Liang, L. Wang and J. Lu, A Novel Super-Toughness and Self-Healing Solid Polymer Electrolyte for Solid Sodium Metal Batteries, *Adv. Mater.*, 2024, **36**, 2409587.

184 I. A. Ojelade, E. Truong, I. P. Oyekunle, T. P. Poudel, Y. Chen, M. J. Deck, Y. Jin, B. Ogbolu, P. K. Ojha, M. M. Islam, T. N. D. D. Gamaralalage, J. S. R. Vellore Winfred and Y.-Y. Hu, Break it down to speed it up: Na2O–NaTaCl6, *Chem. Sci.*, 2025, **16**, 19857–19866.

185 L. Xiang, Y. Gao, Y. Ding, X. Li, D. Jiang, C. Wu, X. Zhan and L. Zhu, Self-forming Na3P/Na2O interphase on a novel biphasic Na3Zr2Si2PO12/Na3PO4 solid electrolyte for long-cycling solid-state Na-metal batteries, *Energy Storage Mater.*, 2024, **73**, 103831.

186 T. Dai, S. Wu, Y. Lu, Y. Yang, Y. Liu, C. Chang, X. Rong, R. Xiao, J. Zhao and Y. Liu, Inorganic glass electrolytes with polymer-like viscoelasticity, *Nat. Energy*, 2023, **8**, 1221–1228.

187 E. Ruoff, S. Kmiec and A. Manthiram, Enhanced Interfacial Conduction in Low-Cost NaAlCl4 Composite Solid Electrolyte for Solid-State Sodium Batteries, *Adv. Energy Mater.*, 2024, **14**, 2402091.

188 Y. Sadikin, M. Brighi, P. Schouwink and R. Černý, Superionic conduction of sodium and lithium in anion-

mixed hydroborates Na3BH4B12H12 and (Li0. 7Na0. 3) 3BH4B12H12, *Adv. Energy Mater.*, 2015, **5**, 1501016.

189 W. S. Tang, M. Matsuo, H. Wu, V. Stavila, A. Unemoto, S.-i. Orimo and T. J. Udovic, Stabilizing lithium and sodium fast-ion conduction in solid polyhedral-borate salts at device-relevant temperatures, *Energy Storage Mater.*, 2016, **4**, 79–83.

190 Y. Lu, L. Li, Q. Zhang, Y. Cai, Y. Ni and J. Chen, High-performance all-solid-state electrolyte for sodium batteries enabled by the interaction between the anion in salt and Na3SbS4, *Chem. Sci.*, 2022, **13**, 3416–3423.

191 S. Kmiec, E. Ruoff, J. Darga, A. Bodratti and A. Manthiram, Scalable Glass-Fiber-Polymer Composite Solid Electrolytes for Solid-State Sodium–Metal Batteries, *ACS Appl. Mater. Interfaces*, 2023, **15**, 20946–20957.

192 Y. Zheng, Y. Yao, J. Ou, M. Li, D. Luo, H. Dou, Z. Li, K. Amine, A. Yu and Z. Chen, A review of composite solid-state electrolytes for lithium batteries: fundamentals, key materials and advanced structures, *Chem. Soc. Rev.*, 2020, **49**, 8790–8839.

193 H. An, M. Li, Q. Liu, Y. Song, B. Deng, X. Liu and J. Wang, Hybrid electrolyte enables solid-state sodium batteries sustaining 50,000 cycles, *Nat Sustainability*, 2025, 1–11.

194 H. Tian, J. Li, Y. Cai, X. Yao and Z. Su, Dendrite-free, interfacially compatible Na 2 ZrCl 6 composite halide solid-state electrolyte for solid-state sodium-ion batteries, *J. Mater. Chem. A*, 2025, **13**, 15178–15188.

195 M. Wang, H. Zhao, B. Du, X. Lu, S. Ding and X. Hu, Functions and applications of emerging metal–organic-framework liquids and glasses, *Chem. Commun.*, 2023, **59**, 7126–7140.

196 W. Tian, G. Lin, S. Yuan, T. Jin, Q. Wang and L. Jiao, Competitive Coordination and Dual Interphase Regulation of MOF-Modified Solid-State Polymer Electrolytes for High-Performance Sodium Metal Batteries, *Angew. Chem., Int. Ed.*, 2025, **64**, e202423075.

197 L. Xiang, D. Jiang, Y. Gao, C. Zhang, X. Ren, L. Zhu, S. Gao and X. Zhan, Self-Formed Fluorinated Interphase with Fe Valence Gradient for Dendrite-Free Solid-State Sodium-Metal Batteries, *Adv. Funct. Mater.*, 2024, **34**, 2301670.

198 R. Wang, W. Feng, X. Yu, Q. Shi, P. Wang, Y. Liu, J. Zhang and Y. Zhao, Stable zero-sodium-excess solid-state batteries enabled by interphase stratification, *eScience*, 2024, **4**, 100274.

199 Y. Lu, Y. Cai, Q. Zhang, L. Liu, Z. Niu and J. Chen, A compatible anode/succinonitrile-based electrolyte interface in all-solid-state Na–CO2 batteries, *Chem. Sci.*, 2019, **10**, 4306–4312.

200 Y. Wang, Z. Wang, F. Zheng, J. Sun, J. A. S. Oh, T. Wu, G. Chen, Q. Huang, M. Kotobuki, K. Zeng and L. Lu, Ferroelectric Engineered Electrode-Composite Polymer Electrolyte Interfaces for All-Solid-State Sodium Metal Battery, *Adv. Sci.*, 2022, **9**, 2105849.

201 E. J. Kim, P. R. Kumar, Z. T. Gossage, K. Kubota, T. Hosaka, R. Tatara and S. Komaba, Active material and interphase structures governing performance in sodium and potassium ion batteries, *Chem. Sci.*, 2022, **13**, 6121–6158.

202 C. Ma, Z. Fu, Y. Fan, H. Li, Z. Ma, W. Jiang, G. Han, H. Ben and H. Xiong, Synergistic interface and structural engineering for high initial coulombic efficiency and stable sodium storage in metal sulfides, *Chem. Sci.*, 2024, **15**, 8966–8973.

203 T. Ortmann, T. Fuchs, J. K. Eckhardt, Z. Ding, Q. Ma, F. Tietz, C. Kübel, M. Rohnke and J. Janek, Deposition of Sodium Metal at the Copper-NaSICON Interface for Reservoir-Free Solid-State Sodium Batteries, *Adv. Energy Mater.*, 2024, **14**, 2302729.

204 L. Li, R. Xu, L. Zhang, Z. Zhang, M. Yang, D. Liu, X. Yan and A. Zhou, O-Tailored Microstructure-Engineered Interface toward Advanced Room Temperature All-Solid-State Na Batteries, *Adv. Funct. Mater.*, 2022, **32**, 2203095.

205 G. Zhao, L. Xu, J. Jiang, Z. Mei, Q. An, P. Lv, X. Yang, H. Guo and X. Sun, COFs-based electrolyte accelerates the Na+ diffusion and restrains dendrite growth in quasi-solid-state organic batteries, *Nano Energy*, 2022, **92**, 106756.

206 L. Gao, J. Chen, Q. Chen and X. Kong, The chemical evolution of solid electrolyte interface in sodium metal batteries, *Sci. Adv.*, 2022, **8**, eabm4606.

207 C. Hänsel, P. V. Kumar and D. Kundu, Stack Pressure Effect in Li3PS4 and Na3PS4 Based Alkali Metal Solid-State Cells: The Dramatic Implication of Interlayer Growth, *Chem. Mater.*, 2020, **32**, 10501–10510.

208 S. Wenzel, T. Leichtweiss, D. A. Weber, J. Sann, W. G. Zeier and J. Janek, Interfacial Reactivity Benchmarking of the Sodium Ion Conductors Na3PS4 and Sodium β-Alumina for Protected Sodium Metal Anodes and Sodium All-Solid-State Batteries, *ACS Appl. Mater. Interfaces*, 2016, **8**, 28216–28224.

209 X. Zhang, Q. J. Wang, B. Peng and Y. Wu, Pressure-Driven and Creep-Enabled Interface Evolution in Sodium Metal Batteries, *ACS Appl. Mater. Interfaces*, 2021, **13**, 26533–26541.

210 J. Suo, Q. Zhao, H. Tian, L. Wang, L. Dai, J. Luo and S. Liu, Designing a Quasi-Liquid Alloy Interface for Solid Na-Ion Battery, *ACS Nano*, 2023, **17**, 10229–10235.

211 S. Cai, H. Tian, J. Liu, S. Liu, L. Dai, J. Xu, L. Kong and L. Wang, Tuning Na3Hf2Si2PO12 electrolyte surfaces by metal coating for high-rate and long cycle life solid-state sodium ion batteries, *J. Mater. Chem. A*, 2022, **10**, 1284–1289.

212 Y. Li, S. Halacoglu, V. Shreyas, W. Arnold, X. Guo, Q. Dou, J. B. Jasinski, B. Narayanan and H. Wang, Highly efficient interface stabilization for ambient-temperature quasi-solid-state sodium metal batteries, *Chem. Eng. J.*, 2022, **434**, 134679.

213 C. Yuan, R. Li, X. Zhan, V. L. Sprenkle and G. Li, Stabilizing Metallic Na Anodes via Sodiophilicity Regulation: A Review, *Materials*, 2022, **15**, 4636.

214 E. Jin, J. Su, H. Hou, P. Pirayesh, Y. Wang, Y. Yuan, H. Yan, G. Popov, L. V. Goncharova, S. Ketabi, F. Dai, C. Cao, L. Chen and Y. Zhao, Electro-Chemo-Mechanically Stable and Sodiophilic Interface for Na Metal Anode in Liquid-based and Solid-State Batteries, *Adv. Mater.*, 2024, **36**, 2406837.

215 X. Luo, J. Mo, X. Xu, F. Li, W. Fan, Y. Wu, J. Zhao, J. Liu and Y. Huo, Interface-Targeting Integrated Sandwich-Structured Na3Zr2Si2PO12 Composite Electrolyte for Ultra-Long Cycle Life Sodium Metal Batteries, *Angew. Chem., Int. Ed.*, 2025, **64**, e202510960.

216 T. Yang, S. Qin, S. Gao, X. Wang, D. Luo, Y. Shi, Q. Ma, X. Zhang, Y. Zhang and Z. Chen, Electroinitiated interfacial healing for external pressure-free solid-state sodium metal batteries, *Nat. Commun.*, 2025, **16**, 9613.

217 Y. Zhang, D. Tie, Z. Xiong, X. Lin, S. Liu, Q. Tan, A. Vlad, M. Xu, Y.-S. Hu and Y. Qi, Fast-Charging Hard Carbons: A Fully Organic SEI Enables Low-Coordination Interfacial Environments and Fast Na+ Desolvation, *Angew. Chem., Int. Ed.*, 2025, **64**, e202516068.

218 S. Xu, C. Xie, R. Wang, H. Sun, D. Sun, X. Meng, H. Zhang, L. Che, Y. Tang and H. Wang, Dispersed Sodophilic Phase Induced Bulk Phase Reconstruction of Sodium Metal Anode for Highly Reversible Solid-State Sodium Batteries, *Adv. Funct. Mater.*, 2025, **52**, e14032.

219 Y. Yang, G. Chang, Z. Liu, X. Chen, C. Huang, Y. Qian, Z. Liu, Q. Tang, A. Hu and X. Chen, Stabilized Solid–Solid Interface for Solid-State Sodium Batteries Using Gradient Ion-Electron Conductive Phases Modified Sodium Metal Anode, *ACS Mater. Lett.*, 2024, **6**, 3564–3571.

220 Z. Sun, Y. Zhao, Q. Ni, Y. Liu, C. Sun, J. Li and H. Jin, Solid-State Na Metal Batteries with Superior Cycling Stability Enabled by Ferroelectric Enhanced Na/Na3Zr2Si2PO12 Interface, *Small*, 2022, **18**, 2200716.

221 X. Li, Q. Zhou, J. Wu, C. Yuan, K. Lu, X. Zhan and L. Zhu, An in Situ Formed Multifunctional Interphase with High Dendrite Tolerance for Long-Life Solid-State Sodium–Metal Batteries, *ACS Appl. Energy Mater.*, 2023, **6**, 10333–10339.

222 L. Zhou, J. D. Bazak, C. Li and L. F. Nazar, 4 V Na Solid State Batteries Enabled by a Scalable Sodium Metal Oxyhalide Solid Electrolyte, *ACS Energy Lett.*, 2024, **9**, 4093–4101.

223 G. Sun, Y. Ma, H. Zhang, S. Wu, S. Chu, S. Passerini and Y. Ma, Fabrication of Composite Cathode for All-Solid-State Sodium Batteries, *Adv. Energy Mater.*, 2025, e03756.

224 Y.-F. Zhu, Y. Xiao, S.-X. Dou, Y.-M. Kang and S.-L. Chou, Spinel/Post-spinel engineering on layered oxide cathodes for sodium-ion batteries, *eScience*, 2021, **1**, 13–27.

225 T. Lan, C.-L. Tsai, F. Tietz, X.-K. Wei, M. Heggen, R. E. Dunin-Borkowski, R. Wang, Y. Xiao, Q. Ma and O. Guillon, Room-temperature all-solid-state sodium batteries with robust ceramic interface between rigid electrolyte and electrode materials, *Nano Energy*, 2019, **65**, 104040.

226 H. Yamauchi, J. Ikejiri, F. Sato, H. Oshita, T. Honma and T. Komatsu, Pressureless all-solid-state sodium-ion battery consisting of sodium iron pyrophosphate glass-ceramic cathode and β″-alumina solid electrolyte composite, *J. Am. Ceram. Soc.*, 2019, **102**, 6658–6667.

227 D. Wang, M. Takiyama, J. Hwang, K. Matsumoto and R. Hagiwara, A Hexafluorophosphate-Based Ionic Liquid as Multifunctional Interfacial Layer between High Voltage Positive Electrode and Solid-State Electrolyte for Sodium Secondary Batteries, *Adv. Energy Mater.*, 2023, **13**, 2301020.

228 W. Meng, J. Liu, L. Wang, L. Dai and S. Liu, In Situ Construction of a Liquid Film Interface with Fast Ion Transport for Solid Sodium-Ion Batteries, *Nano Lett.*, 2022, **22**, 5214–5220.

229 C. M. Costa, Y.-H. Lee, J.-H. Kim, S.-Y. Lee and S. Lanceros-Méndez, Recent advances on separator membranes for lithium-ion battery applications: From porous membranes to solid electrolytes, *Energy Storage Mater.*, 2019, **22**, 346–375.

230 J. Wu, S. Liu, F. Han, X. Yao and C. Wang, Lithium/Sulfide All-Solid-State Batteries using Sulfide Electrolytes, *Adv. Mater.*, 2021, **33**, 2000751.

231 H. Zhang, Y. Zhang, D. Yan, P. Lv, C. Yu, H. Zheng, L. Yan, Z. Cheng, H. Y. Yang and Y. Bai, Activating Ferroelectric-Magnetic Synergistic Effects at Cathode-Electrolyte Interfaces Toward Superfast and Stable Sodium Storage, *Adv. Mater.*, 2025, **37**, e02846.

232 J.-C. Liu, T. You, Y.-F. Zhao, F.-Q. Liu, J.-D. Li, L.-L. Wang, C. Wang and L. Li, Multifunctional sulfonate additive induced CEI layer enables ultra-stable PEO based solid-state sodium batteries, *Rare Met.*, 2025, **44**, 3817–3826.

233 M. Hou, J. Zi, L. Zhao, Y. Zhou, F. Li, Z. Xie, D. Zhang, B. Yang and F. Liang, Enhancement of interfacial sodium ion transport stability in quasi-solid-state sodium-ion batteries using polyethylene glycol, *Mater. Chem. Front.*, 2023, **7**, 2027–2037.

234 L. Lu, Y. Lu, J. A. Alonso, C. A. López, M. T. Fernández-Díaz, B. Zou and C. Sun, A Monolithic Solid-State Sodium–Sulfur Battery with Al-Doped Na3.4Zr2(Si0.8P0.2O4)3 Electrolyte, *ACS Appl. Mater. Interfaces*, 2021, **13**, 42927–42934.

235 H. Lai, Y. Li, J. Wang, W. Li, X. Wu and Z. Wen, Design of solid-state sodium-ion batteries with high mass-loading cathode by porous-dense bilayer electrolyte, *J. Materiomics*, 2021, **7**, 1352–1357.